

İSTANBUL TEKNİK ÜNİVERSİTESİ★ FEN BİLİMLERİ ENSTİTÜSÜ

75456

## ELASTİK ROTOR PALLERİNİN FREKANS EŞİTLİKLİ OPTİMİZASYONU

Yük.Lis. Tezi  
Mak.Müh. HÜLYA BULUR

75456

Tezin Enstitüye Verildiği Tarih : 8. Haz. 1998  
Tezin Savunulduğu Tarih : 26. Haz. 1998

Tez Danışmanı  
Diğer Jüri Üyeleri

: Doç.Dr.Y.Kemal YILLIKÇI  
: Prof.Dr.Süleyman TOLUN  
Yrd.Doç.Dr.Reşat Kürem

23.07.1998  
23.7.1998  
12.8.1998

YÜKSEKÖĞRETİM ENSTİTÜSÜ  
İSTANBUL TEKNİK ÜNİVERSİTESİ

HAZİRAN 1998

**ISTANBUL TECHNICAL UNIVERSITY ★ NATURAL SCIENCES INSTITUTE**

**OPTIMUM DESIGN OF ROTOR BLADES WITH EQUALITY  
CONSTRAINT**

**M. Sc. THESIS  
MECHANICAL E. HÜLYA BULUR**

**Date of Submission : June 8, 1998**

**Date of Approval : June 26, 1998**

**Thesis Adviser**

**Jury**

**Jury**

**: Assoc.Prof.Dr.Y.Kemal YILLIKCI**  23.07.98

**: Prof.Dr.Süleyman TOLUN**  23.7.1998

**: Assoc.Prof.Dr.Reşat Kürem**  12.8.1998

**JUNE 1998**

## ACKNOWLEDGEMENT

The problem of minimum weight design of a helicopter rotor blade subject to a constraint on its first coupled flap-lag-torsional natural frequency has been studied in this paper. Modern structural optimization technique based on optimality criteria approach has been applied for optimizing the weight of the blade. Optimum designs are presented for a typical soft and stiff-in-plane hingeless rotor configurations. The results indicate that the application of structural optimization techniques lead to benefits in rotor blade design not only through substantial reduction in weight but a considerable reduction in the vibratory hub shears and moments at the blade root due to proper placement of blade natural frequency.

I thank to my teacher Doç.Dr. Yıldırım Kemal YILLIKÇI who doesn't withhold his knowledge and helps from me during my study and also I thank , first, to my family, my friends who support me all the time.

## **CONTENTS**

	<b>PAGE</b>
<b>ACKNOWLEDGEMENT</b>	II
<b>LIST OF SYMBOLS</b>	IV
<b>LIST OF FIGURES</b>	VII
<b>LIST OF TABLE S</b>	IX
<b>ÖZET</b>	X
<b>SUMMARY</b>	XI
<b>CHAPTER 1 INTRODUCTION</b>	1
1.1 Rotor Blades Aeroelastic Tailoring: Multivariable Optimazing Problem	1
1.2 Mathematical Formulation: Optimization	5
1.2.1 Background on Optimum Design with Frequency Constraints	5
<b>CHAPTER 2 PROBLEM FORMULATION</b>	6
2.1 Discretization of the Equations of Motion Using the Galerkin Finite Element Method	8
2.2 Formulation of Equality Frequency Constraints Problem	10
2.2.1 Formulation of the Optimization Problem	13
2.2.2 Recursion Relations	16
<b>CHAPTER 3 RESULT ARE DISCUSSION</b>	20
3.1 Configuration Definitions	20
3.2 Numerical Results For Selected Rotorblade Configurations	23
3.2.1 Soft Inplane Hingeless Rotor Blade	23
3.2.2 Hingeless Rotor Blade	26
<b>REFERENCES</b>	35
<b>APPENDIX A</b>	40
<b>APPENDIX B</b>	46
<b>APPENDIX C</b>	52
<b>CIRCULURIUM VITA</b>	54

## LIST OF SYMBOLS

- $K$  = Unsymmetrical matrix  
 $W$  = Total Weight of the resulting diacritized blade  
 $\rho_{ei}$  = Material Density  
 $i_{ei}$  = Element length  
 $A_{ei}$  = Cross sectional area  
 $\phi_n$  = Design variable  
 $\omega_K$  = Frequency  
 $q_k$  = Eigenvector of the rotor blade  
 $\mu$  = LaGrange Multiplier  
 $\beta$  = Relaxation parameter  
 $\alpha$  = Positive Exponent  
 $\omega$  = Equality Constraint of the desired frequency  
 $I_m$  = Mass Moment of inertia of the blade cross section  
 $m_{ns}$  = Mass per unit length  
 $a$  = two dimensional lift curve slope  
 $a_n^e$  = Element nodal parameters  
 $a^e$  = Element nodal displacement vector  
 $\alpha$  = system nodal displacement vector  
 $[A^K]$  = Aerodynamic operator and stiffness Matrix  
 $[A_1]$  = Aerodynamic operator and stiffness Matrix  
 $[A_2]$  = Aerodynamic operator and stiffness Matrix

$[A_1^c]$  = Aerodynamic operator and stiffness Matrix

$[A_2^c]$  = Aerodynamic operator and stiffness Matrix

$[A_3^c]$  = Aerodynamic operator and stiffness Matrix

$b_m$  = Modal parameters

$\{b_m\}$  = Vector of Modal parameters

$\bar{b} = \frac{b}{R}$  = Air foil semi-cord

$[B]$  = Binding Stiffness operator and matrixes

$[B^c]$  = Binding Stiffness operator and matrixes

$[B_1^c]$  = Element Stiffness matrix

$[B_2^c]$  = Element Stiffness matrix

$[B_c^c]$  = Boundary condition term due to route torsional stiffness

$B_{22}$  = Non-dimensional biding rigidities

$B_{23}$  = Non-dimensional biding rigidities

$B_{33}$  = Non-dimensional biding rigidities

$B_4$  = Non-dimensional biding rigidities

$B_{m22}$  = Non-dimension mass moment of inertia

$B_{m23}$  = Non-dimension mass moment of inertia

$B_{m33}$  = Non-dimension mass moment of inertia

$B_{m4}$  = Non-dimension mass moment of inertia

$B_{m0}$  = Non-dimension mass moment of inertia

$C_{d0}$  = Blade profile drag coefficient

$\hat{e}_x \hat{e}_y \hat{e}_z$  = Unit vector triad in  $x_0, y_0, z_0$  direction respectively before deformation

$\hat{e}'_x \hat{e}'_y \hat{e}'_z$  = Unit vector triad in  $e_x, e_y, e_z$  direction respectively after deformation

$E$  = number of finite element

$\theta_f$  = element torsion displacement

$F_1, F_2, F_3, F_4$  = coefficients in the aerodynamic loads

$F_5$

- $F$  = Known Function
- $\tilde{g}^e, g_n^e$  = element flap displacement
- $g_m$  = generalized coordinates,  $m^{\text{th}}$  flap mode
- $GJ$  = Blade torsional rigidity,  $GJ = GJ/(m_0 \Omega^2 l^4)$
- $\tilde{h}, h_n^e$  = element lag displacement
- $h_m$  = generalized coordinate,  $m^{\text{th}}$  lag mode
- $I_2, I_3$  = principal moment of inertia for lagwise and flapwise bending
- $I_b$  = blade mass moment of inertia in flap
- $I_{m2}, I_{m3}$  = cross sectional mass moment of inertia
- $I_{m2} = I_{m2} / (m_0 l^2), I_{m3} = I_{m3} / (m_0 l^2),$
- $K_\phi$  = root torsional spring stiffness
- $l$  = length of elastic portion of blade
- $\bar{m} = \frac{m}{m_0}$  = mass per unit length of the blade
- $m_0$  = reference value for mass per unit length of the blade
- $M_x, M_1, M_2, M_3$  = elastic moments, non- dimensional
- $N$  = number of element shape function for each elastic degree of freedom
- $\tilde{p}$  = distributed external force vector per unit length of blade non-dimensional, subscripts I, A and D represent inertia, aerodynamic and structural damping contributions
- $P$  = differential operator
- $\tilde{v} = \frac{v}{l}$  = elastic lag displacement
- $\tilde{w} = \frac{w}{l}$  = elastic flap displacement
- $\tilde{x}_e = \frac{x_e}{l}$  = element coordinate

- $\beta_p$  = blade precone, inclination of the feathering axis with respect to the hub plane
- $\gamma$  = lock number
- $\Gamma$  = coefficient
- $\varepsilon$  = residual
- $\rho$  = mass density of blade material
- $\sigma$  = solidity ratio
- $\phi$  = elastic torsion deformation
- $\phi_m$  = global shape function
- $\zeta_n^e$  = element shape function
- $\tilde{\eta} = \{\eta_n\}$  = vector of element flap interpolation polynomials





## LIST OF FIGURES

	PAGE
Figure 2.1: Box Beam Structure Geometry	7
Figure 2.2: Beam Type Finite Element and the Associated Degrees of Freedom	12
Figure 3.1: Results for Soft Inplane Configuration, $\phi_{\min}/\phi_{ini} = 1/8$	27
Figure 3.2: Results for Soft Inplane Configuration, $\phi_{\min}/\phi_{ini} = 1/4$	28
Figure 3.3 : Results for Soft Inplane Configuration, $\phi_{\min}/\phi_{ini} = 1/2$	29
Figure 3.4 : Results for Stiff Inplane Configuration, $\phi_{\min}/\phi_{ini} = 1/12$	31
Figure 3.5 : Results for Stiff Inplane Configuration, $\phi_{\min}/\phi_{ini} = 1/3$	32
Figure 3.6 : Results for Stiff Inplane Configuration, $\phi_{\min}/\phi_{ini} = 1/6$	33

## LIST OF TABLES

	PAGE
Table 3.1: Configuration Parameters for Flap-Lag-Torsion Motions in Hover	23
Table 3.2 : Cross Sectional Properties of the Box Beam Structure	26
Table 3.3: Optimization Results for the Soft Inplane Configuration	26
Table 3.4: Optimization Results for the Stiff Inplane Configuration	30



## ÖZET

### ELASTİK ROTOR PALLERİNİN FREKANS EŞİTLİKLİ OPTİMİZASYONU

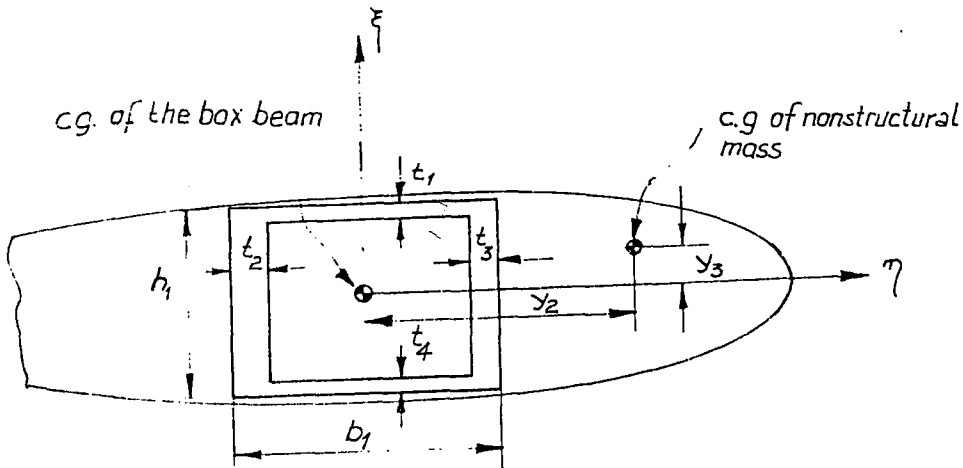
Bir helikopter palinin tasarımında, gözönünde bulundurulan kriter, doğal frekanslarının yer ve hava rezonansından koruyacak şekilde düşünülmesidir.

Bu çalışmada, yer rezonansından korunmak için birinci doğal frekansı sabit tutarak, rotor palinin ağırlığının optimum yapılması üzerinde durulmuştur.

Rotor palinin hareket denklemleri, Galerkin sonlu elemanlar yöntemiyle ayrıştırılmış ve en genel halde aşağıdaki şekilde yazılmıştır:

$$M\ddot{q} + (C + \hat{C})\dot{q} + (K_s + K_a)q = f(t)$$

Rotor palinin kesiti aşağıdaki şekilde dikdörtgen çekirdekten ibaret olduğu kabul edilmiştir. Optimizasyon esnasında tasarım değişkeni olarak -b- boyutu kullanılmıştır. Palin hareket denklemleri, Lagrange çarpanları kullanılarak çözümlenmiştir. Üretimi mümkün olmayan tasarım değerleri elde etmemek için , tasarım değişkeni belirli değerler arasında tutulmuştur. Yapılan kabuller ise, palin ankastre olduğu, sönümsüz hareketin mevcudiyetidir.



Palin dikdörtgen kesiti

## SUMMARY

### OPTIMUM DESIGN OF ROTOR BLADES WITH EQUALITY CONSTRAINT

#### 1.PROBLEM FORMULATION

An important design of helicopter rotor blades is the placement of the natural frequencies to avoid ground and air resonances. This is done by proper tailoring of the blade mass of the stiffness distribution to give a set of desired natural frequencies. However, this is not an easy task due to the presence of various coupling effects as discussed in Reference [38]. The pitch angle, blade twist and an off-set between the elastic and inertia axes generally cause linear coupling effects between natural modes of the rotor blades. The scope of the present study is to find a suitable mass distributions of the blade which minimizes the weight while holding the selected natural frequency at a specified value. Minimum bound limits are imposed on the selected design variables to prevent them from reaching impractical values during the design optimization process.

Figure 1.1 depicts a typical rotor blade with a thin walled box beam cross section along the span and leading edge tuning masses distributed along the span. In order to simplify the analysis the following assumptions are made. The stiffness of the blade is contributed by the unsymmetric box section with variable geometry and nonstructural mass distribution along the span. Stiffness contributed by skin, etc. is negligible. The material density is assumed to be uniform throughout the blade. For the structural analysis of the box beam, warping effects are neglected and thin wall approximations are used. The simplified problem is formulated as to minimize the weight of the blade which is assumed to be the sum of the weights of the box beam and the distributed tip tuning masses. This is also called as the objective function. Any combinations of the box beam dimensions  $b, h, t_1, t_2, t_3$  can be used as the design variable. The governing equations of motion of hingeless rotor blades are formulated in different references. Different methods are used to discretize these

equations. In this study, the discrete parameter form of the rotor blade equations are given

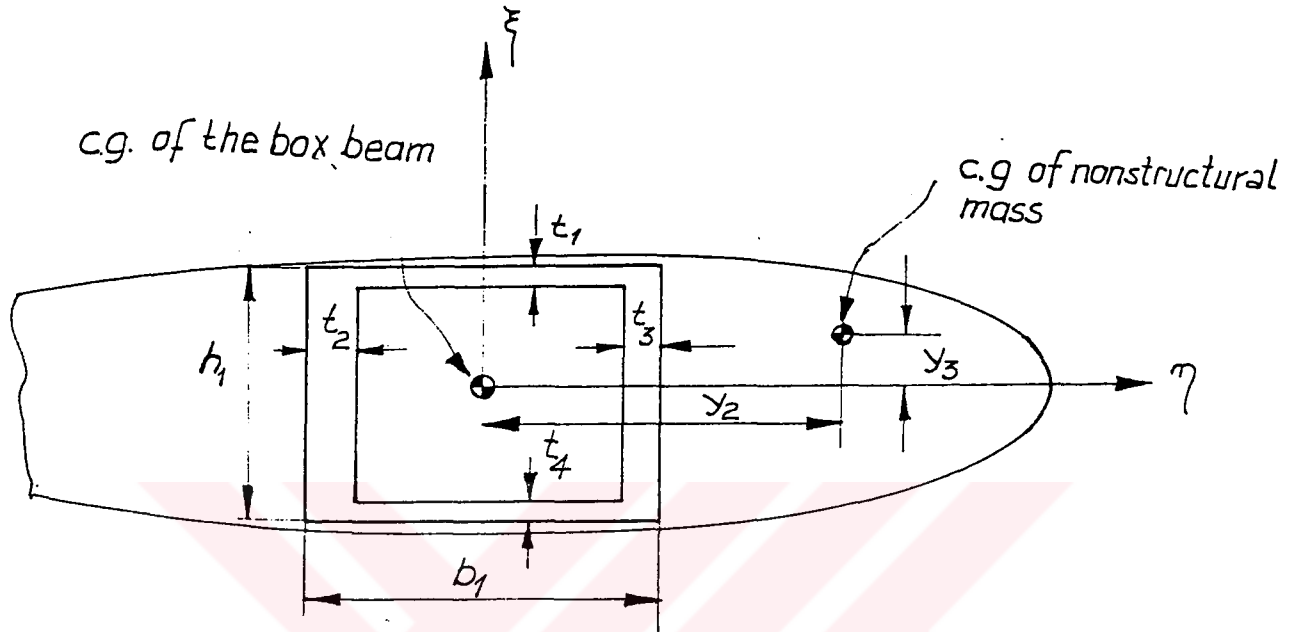


Figure 1.1: Box Beam Structure Geometry

by reference [44]. These equations are discretized by Galerkin type finite element method and are for general coupled flap-lag-torsion dynamics of a hingeless rotor blade both for forward and hover flight conditions with arbitrary mass and stiffness distributions. Cross sectional mass center and aerodynamic center offsets from the elastic axis are also included. Quasisteady aerodynamics has been used in developing the equations where the compressibility and stall effects are not included. The problem of weight minimization subject to a constraint on a natural frequency is often referred as to the dual problem. The primal problem is the one where the natural frequency is maximized holding the weight to a specified value. Both of these problems as applied to optimum design of nonrotating beams with thin-walled cross sections undergoing coupled bending and torsional vibrations have been addressed by

Hanagud and Chattopadhyay [23,24]. It has been observed that the optimum distributions differ largely with and without the coupling effects.

### 1.1 Discretization of the Equations of Motion Using the Galerkin Finite Element Method□

□

The first step in solving the equations of motion is the discretization of the spatial dependence. This is accomplished through application of the Galerkin finite element method. Subsequently, modal analysis is used to reduce the number of discrete unknowns describing the problem.

### 1.2 Formulation of Equality Frequency Constraints Problem

The discrete parameter form of the governing equation of the rotor blade motion is given by Reference [44] as

$$M\ddot{q} + (C + \hat{C})\dot{q} + (K_S + K_A)q = f(t) \quad (1.1)$$

in above equation,  $K = K_S + K_A$  is a real unsymmetric matrix where indices S and A corresponds to structural and aerodynamic effects respectively. Finite element used to discretize the blade and the associated degrees of freedoms are shown in Figure 1.2. In this simplified analysis rotor blade motion in hover case is considered. The linear undamped motion of the rotor blade is given by

$$M\ddot{q} + (K_S + K_A)q = f(t) \quad (1.2)$$

Elemental degrees of freedoms are rearranged such that,

$$q^e = \{v_1, v'_1, w_1, w'_1, \phi_1, v_2, v'_2, w_2, w'_2, \phi_2\}^T$$

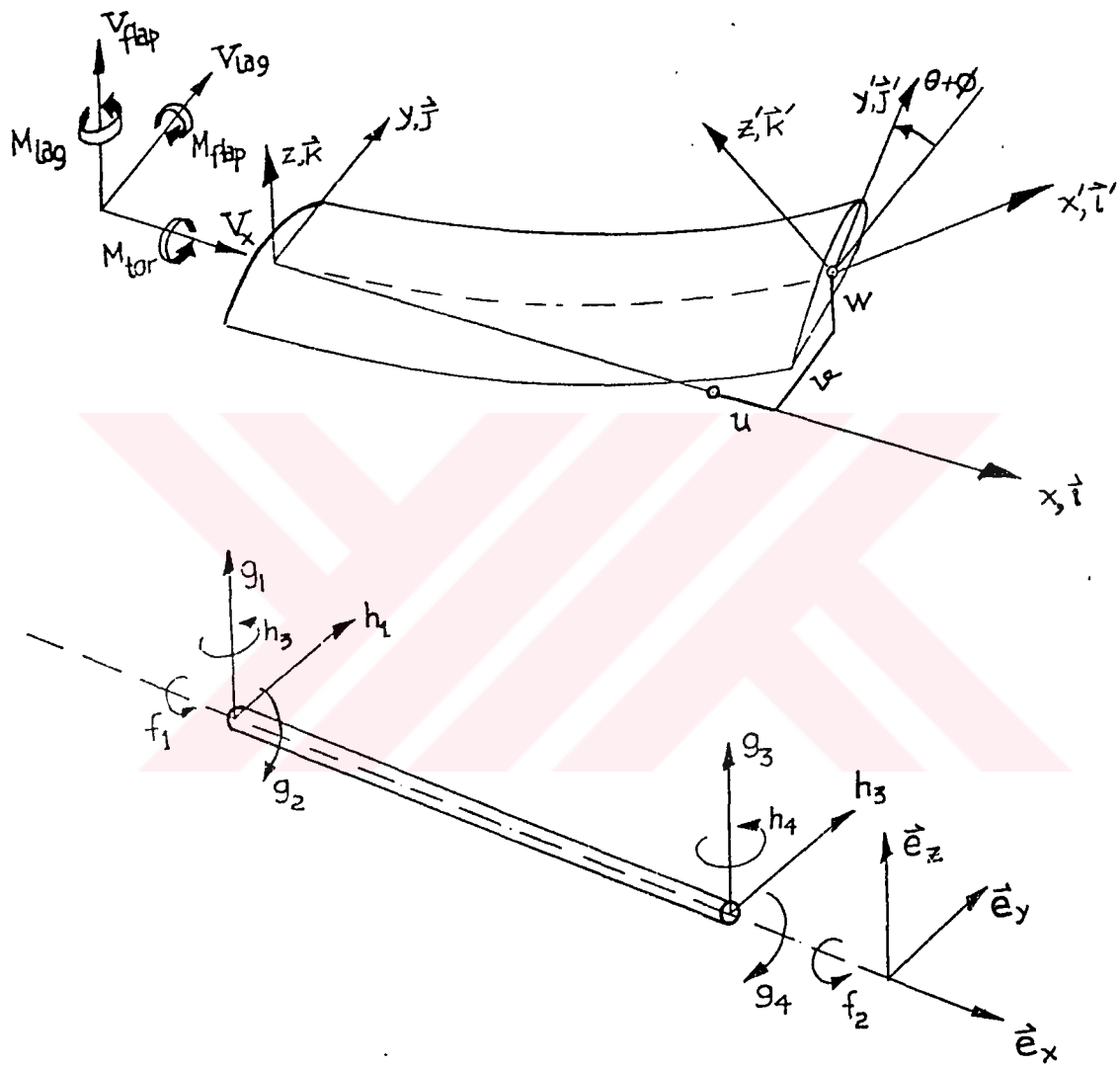


Figure 1.2: Beam Type Finite Element and Associated Degrees of Freedom

The eigenvalue problem of the nonsymmetric system can be written as [45].

$$\begin{aligned} (K - \omega_i^2 M) q_i &= 0 \\ (K^T - \omega_i^2 M^T) s_i &= 0 \end{aligned} \quad (1.3)$$

where  $q_i$  and  $s_i$  are defined as right and left eigenvectors corresponding to the  $i$ th eigenvalue,  $\omega_i^2$ . Both sets of eigenvectors can be expressed as square matrices  $Q$  and  $S$  as

$$\begin{aligned} Q &= [q_1, q_2, \dots, q_n] \\ S &= [s_1, s_2, \dots, s_n] \end{aligned} \quad (1.4)$$

and orthonormality conditions can be also written as,

$$\begin{aligned} S^T M Q &= [I] \\ S^T K Q &= [\Lambda] \end{aligned} \quad (1.5)$$

where  $\Lambda$  is a diagonal matrix with eigenvalues on its diagonals.

### 1.1.1 Formulation of the Optimization Problem

The total weight of the resulting discretized blade is

$$W = \sum_{i=1}^{n_e} (\rho_{e_i} l_{e_i} A_{e_i} + W_{t_i}) \quad (1.6)$$

where,  $\rho_{e_i}$ , is the material density,  $l_{e_i}$ , is the element length,  $A_{e_i}$ , is cross sectional area and  $W_{t_i}$  is the nonstructural mass. The optimization problem can now be posed as follows:

Minimize:



$$W = \sum_{i=1}^n (\rho l A + W) \quad (1.7)$$

Subject to:

Equilibrium condition;

$$\begin{aligned} (K - \omega_k^2 M) q_k &= 0 \\ (K^T - \omega_k^2 M^T) s_k &= 0 \end{aligned} \quad (1.8)$$

Orthonormality condition;

$$\begin{aligned} s_k^T M q_l &= \delta_{kl} \\ s_k^T K q_l &= \delta_{kl} \omega_{kl} \end{aligned} \quad (1.9)$$

Besides design variables are bounded by lower and upper limits;

$$\phi_{\min} \leq \phi_n \leq \phi_{\max} \quad (1.10)$$

As a first step only the problem of unsymmetric matrices and the associated frequency constraints are considered. As the next step, the constrained optimization problem is now converted into an unconstrained one by the use of Lagrange multipliers. The modified objective function is written as

$$\begin{aligned} W^* &= \sum_{i=1}^n (\rho_{e_i} l_{e_i} A_{e_i} + W_{t_i}) \\ &-- \mu_1 (s_k^T K_{e_i} q_k - \omega_k^2) - \mu_2 (q_k^T K_{e_i}^T s_k - \omega_k^2) \\ &- \nu_1 (s_k^T M_{e_i} q_k - 1) - \nu_2 (q_k^T M_{e_i}^T s_k - 1) \\ &- \Omega_1 (K_{e_i} - \omega_k^2 M_{e_i}) q_k - \Omega_2 (K_{e_i}^T - \omega_k^2 M_{e_i}^T) s_k \end{aligned} \quad (1.11)$$

In above equation  $\omega_k$  is the frequency which is desired to set equal to the  $\nu$ ,  $s_k$  and  $q_k$  are the corresponding eigenvectors of the rotor blade system. The problem now is to minimize  $W^*$  subject to the constraints on the design variables. The se constraints are given by equation 1.10. This is done by obtaining stationary value of the objective function  $W^*$  using full resources of variational techniques, While staying within the bounds on the design variables.

The necessary condition for the stainerity is given by,

$$\Delta W^* = 0 \quad (1.12)$$

This leads to the condition,

$$\begin{aligned} \frac{\partial W^*}{\partial q_1} &= 0 \\ \frac{\partial W^*}{\partial s_1} &= 0 \end{aligned} \quad (1.13)$$

In view of equation 1.3 and 1.9, these conditions yiel to

$$\begin{aligned} \Omega_1 &= -(\mu_1 + \mu_2) s_1 \\ \Omega_2 &= -(\mu_1 + \mu_2) q_1 \end{aligned} \quad (1.14)$$

and

$$\nu_1 + \nu_2 = -\omega_i^2 (\mu_1 + \mu_2) \quad (1.15)$$

The next requirement is  $\frac{\partial W^*}{\partial \phi_i} = 0$  and can be derived from equation 1.11. This

follows a set of optimality criteria condition given below,

$$\frac{\partial W^*}{\partial \phi_n} = \rho_{e_i} l_{e_i} \frac{\partial A_{e_i}}{\partial \phi_n}$$

$$\begin{aligned}
- & \mu_1 \left( s_{k_i}^T \frac{\partial K_{e_i}}{\partial \phi_n} q_{k_i} \right) - \mu_2 \left( q_{k_i}^T \frac{\partial K_{e_i}^T}{\partial \phi_n} s_{k_i} \right) \\
- & \nu_1 \left( s_{k_i}^T \frac{\partial M_{e_i}}{\partial \phi_n} q_{k_i} \right) - \nu_2 \left( q_{k_i}^T \frac{\partial M_{e_i}^T}{\partial \phi_n} s_{k_i} \right) \\
- & \Omega_1^T \left( \frac{\partial K_{e_i}}{\partial \phi_n} - \omega_k^2 \frac{\partial M_{e_i}}{\partial \phi_n} \right) q_{k_i} - \Omega_2^T \left( \frac{\partial K_{e_i}^T}{\partial \phi_n} - \omega_k^2 \frac{\partial M_{e_i}^T}{\partial \phi_n} \right) s_{k_i}
\end{aligned} \tag{1.16}$$

Using equations 1.14, 1.15, 1.16 the optimality condition is rewritten as

$$\frac{\partial A_i}{\partial \phi_n} \rho_{e_i} l_{e_i} - \mu \left( \omega_k^2 s_{k_i}^T \frac{\partial M_{e_i}}{\partial \phi_n} q_{k_i} - s_{k_i}^T \frac{\partial K_{e_i}}{\partial \phi_n} q_{k_i} \right) = 0 \quad i = 1, 2, \dots, n_i \tag{1.17}$$

where  $n_i$  denotes the number of elements over which the design variable  $\phi_i$  does not reach the limiting values posed by equation 1.10. Note that the global mass and stiffness matrices  $M$  and  $K$  are replaced by the corresponding elemental quantities  $M_{e_i}$  and  $K_{e_i}$  respectively,. Similary eigenvectors  $q_k$  and  $s_{k_i}$  are also replaced by corresponding elemental eigenvectors  $q_K$  and  $s_K$ . This has been done since there exist a one to one correspondence between an element and a design variable or in other words,  $\phi_n$ , only appears in the element stiffness and mass matrices of the  $i$ th element. A simultaneous solutions of equations 1.7, 1.8, 1.9, and equation 1.17 with in the bounds equation 1.10 will result in possible optimum designs.

## **CHAPTER 1**

### **INTRODUCTION**

#### **1.1 ROTOR BLADES AEROELASTIC TAILORING: MULTIVARIABLE OPTIMIZATION PROBLEM**

Many different considerations are necessary in designing a helicopter rotor blade. Some of these considerations include strength, damage tolerance, fatigue life reliability and survivability. However, a very important design consideration is the requirement of separating the natural frequencies of the blades from the aerodynamic forcing frequencies to avoid resonance. This is done by a proper tailoring of the blade mass or the stiffness distribution to give a set of desired natural frequencies. However, this is not an easy task due to the presence of various coupling effects as discussed in reference [1]. One such reason is that the natural modes of the rotor blade twist, large aerodynamic damping and offset between the elastic and inertial axes. The problem is further complicated by margins less than 20 percent in the range of importance. A failure to consider frequency placement at the stage of the preliminary design has the potential of significantly increasing the weight in the structure. However, most of the present preliminary design practices are not to tailor the design and place the desired natural frequencies. After the design is completed, the designer checks for poorly placed natural frequencies and corrects for these poor placements by placing appropriate nonstructural masses at crucial locations.

In order to avoid such weight penalties, as explained by Peters [2], it is now possible to design and fabricate a helicopter blade that includes appropriate prescribed variations in stiffness which permit placements of frequencies at the preliminary design stages. One of the reasons for this possibility is as follows. Rotor blades are being fabricated by the use of composite materials. The state of art of structural dynamic system optimization techniques and parameter identification techniques have improved to a state such that it is possible to apply these techniques at the preliminary

design stage of rotor blade and obtain appropriate variations in stiffnesses that results in desired placement of natural frequencies.

## 1.2 BACKGROUND

Significant developments in the field of the application of optimization techniques to rotor blade designs can be traced to the works of Bielawa [3], Bennett [4,5], Friedmann [7,6], Peters [2], and Taylor [8]. Bielawa [3] has developed an optimization procedure to reduce blade loads consisted with aeroelastic restraints. This method, however, was not completely automated. Taylor has considered the problem by the use of modal shaping. The objective of his work is to reduce vibration levels by modifying the mass and stiffness distributions in order to modify modal shape parameters. These modal shape parameters have been sometimes interpreted as an ad-hoc optimality criterion. A very brief summary of other works due to Bennett, Friedmann and Peters are outlined as follows.

Bennett [4,5] has considered problems of minimizing hub shears and blade weight. However, in this study, the contribution of aerodynamics to stiffness and damping are neglected in obtaining frequency constraints. It is equivalent to considering the system in vacuum. Friedmann [7,6] has considered the problem of minimizing hub shears or hub vibratory rolling moments subject to aeroelastic and frequency constraints. These aeroelastic constraints are based on a fully coupled analysis of coupled flap-lag-torsional analysis of the rotor blade. However, the frequency constraints of the problem are based on the uncoupled modes.

Peters [2] has addressed the problem of the placement of frequencies alone. Similarly the blade was assumed to be in vacuum but c.g offset from the elastic axis and twist are included to the problem. The problem of multiple frequency constraints are reduced to a single objective function. This study, based on coupled analysis of frequencies, has been formulated with inequality constraints for frequency placements. This has been motivated by the difficulties associated with handling equality constraints by nonlinear mathematical programming techniques like Conmin.

Following these studies, several aspects of rotor blade optimization have been investigated : Walsh [9] developed a formal optimization procedure for helicopter rotor blade designs which minimizes hover horsepower while assuring satisfactory forward flight performance. Lim and Chopra [11] developed a structural optimization procedure for a hingeless rotor to reduce oscillatory hub loads while maintaining aeroelastic stability in forward flight. In these study a wide range of design variables including distribution of nonstructural mass, chordwise location of blade c.g., blade bending stiffness are used as the design variables to structurally optimize the blade. Sensitivity derivatives of blade responses , hub loads and eigenvalues with respect to design variables are derived by the use of a direct analytical approach which reduced the computational time substantially.

Recently, Banerje and Shanthakumaran [12] reviewed applications of numerical optimization methods in helicopter industries. As stated in this review, helicopter optimization process is a multilevel approach, which consist of a global level and a local level , is used to achieve an overall optimum helicopter configuration. As the general approach at the global level the overall configuration of the helicopter is aimed to be optimized to meet the mission requirements. At the local level the preliminary components are optimized to meet their specific design requirements. Particularly, for rotor blade optimization studies these primary optimizations are aimed (i) the rotor blade airfoil profile is optimized to improve performance [13] (ii) the structural properties of the rotor blades are aeroelastically tailored to improve performance, properly place the blade frequencies, minimize blade and hub loads; or minimize the blade weight [2,4,5,6,7,8,3,11] (iii) the rotor blade geometry is optimized for performance both in hover and forward flight [9,10,14] (iv) the bearingless rotor hub structurally tailored for cyclic stresses causing fatigue and crack propagation [15].

These separate level optimizations have several common design parameters. A design variable which is obtained for a local optimization process may fall into a very undesirable range of variables for the optimum solution of another local goal. In present these local level optimization processes are coordinated with each other by engineering judgements based on the experiences of the design team.

In future applications, global optimizations of rotor blades can be achieved by a highly automated global procedure which will be using a combination of several local level optimizations. This coordination between these local level optimizations will guide individual processes so the critical design variables are globally optimized. As discussed before, these critical design variables tend to give different optimum values at different local level optimizations. In current applications these design variables are constrained for different local levels and for global solutions they are iterated between these local level optimizations.

As a future goal this procedure can be guided by an expert system based on artificial intelligence techniques. For this type of a global optimization local level optimizations must be integrated by each other such away that they will share informations about the optimizations trends at each separate local procedures. This share of trend information will help the expert system to guide each local level optimizations to proceed such that they can optimize the critical design variables to common global optimum values.

Current minimum design processes of helicopter rotor blades generally uses package programs like CONMIN for the optimization processes. On the other hand the integration of local level optimizations and optimization trend information generations require the use of explicitly formulated optimization procedures. This new approach brings the necessity to develop local level optimization procedures which are specially formulated for the specified problem. In view of this new approach, Hanagud [22] attempted to extend a previously developed [23,24] optimization method for rotor blades frequency placement and blade weight minimization. This paper, is extension of optimum design problem of placement of natural frequencies has been formulated with equality constraints on frequencies and a minimum weight objective [22].

The intended procedure is to consider the minimization problem with one frequency constraint at each time. Aerodynamic forces and moment and the effect of the aerodynamics on the stiffness of the system is included to the problem but both structural aerodynamic damping effects are neglected for the initial study. The problem is formulated such away that it can handle mass center offset from the elastic

axis. The optimization is based on an optimality criterion that can consider equality constraints with little difficulty. A purpose of selecting this reduced problem is to understand the problem of frequency placement first and then consider the problem of combined frequency and aeroelastic constraints by the use of optimality criterion approach studies.

## **1.2 MATHEMATICAL FORMULATION:OPTIMIZATION**

### **1.2.1 Background on Optimum Design with Frequency Constraints**

The problem considered in this paper falls in the category of optimum design of beam problems with frequency constraints. The first investigation of the beam vibration problem is attributed to Niordson [25]. He considered the problem of finding the best taper that yields the highest possible natural frequency. Following the initial work of Niordson, many different investigations have considered different problems in the field of optimal vibration of beams. References [26,27,28,29,30,31] [12-17] deal with the problem of maximization of fundamental frequencies. The problem of maximizing higher order frequencies and rotating beams was addressed by Olhoff [32,33,34]. The problem of minimizing weight for a specified frequency constraints has been addressed in References [35,26,37,38,39,40]. Multiple frequency constraints have been also addressed in References [41,42,43]. An optimality criteria approach has been discussed in References [39,41].

The work of this paper is also based on the optimality criterion approach. However, all the aforementioned works have considered reciprocal relationships and symmetric stiffness matrices. The problem considered here does not always have symmetric stiffness matrix because of the aerodynamic contributions to the stiffness of the system. The optimality criterion has been derived by the use of biorthogonal eigenvectors



## CHAPTER 2

### PROBLEM FORMULATION

As discussed in the previous sections, an important design of helicopter rotor blades is the placement of the natural frequencies to avoid ground and air resonances. This is done by proper tailoring of the blade mass of the stiffness distribution to give a set of desired natural frequencies. However, this is not an easy task due to the presence of various coupling effects as discussed in Reference [38]. The pitch angle, blade twist and an off-set between the elastic and inertia axes generally cause linear coupling effects between natural modes of the rotor blades. The scope of the present study is to find a suitable mass distributions of the blade which minimizes the weight while holding the selected natural frequency at a specified value. Minimum bound limits are imposed on the selected design variables to prevent them from reaching impractical values during the design optimization process.

Figure 2.1 depicts a typical rotor blade with a thin walled box beam cross section along the span and leading edge tuning masses distributed along the span. In order to simplify the analysis the following assumptions are made. The stiffness of the blade is contributed by the unsymmetric box section with variable geometry and nonstructural mass distribution along the span. Stiffness contributed by skin, etc. is negligible. The material density is assumed to be uniform throughout the blade. For the structural analysis of the box beam, warping effects are neglected and thin wall approximations are used. The simplified problem is formulated as to minimize the weight of the blade which is assumed to be the sum of the weights of the box beam and the distributed tip tuning masses. This is also called as the objective function. Any combinations of the box beam dimensions  $b, h, t_1, t_2, t_3$  can be used as the design variable.

The governing equations of motion of hingeless rotor blades are formulated in different references. Different methods are used to discretize these equations. In this study, the

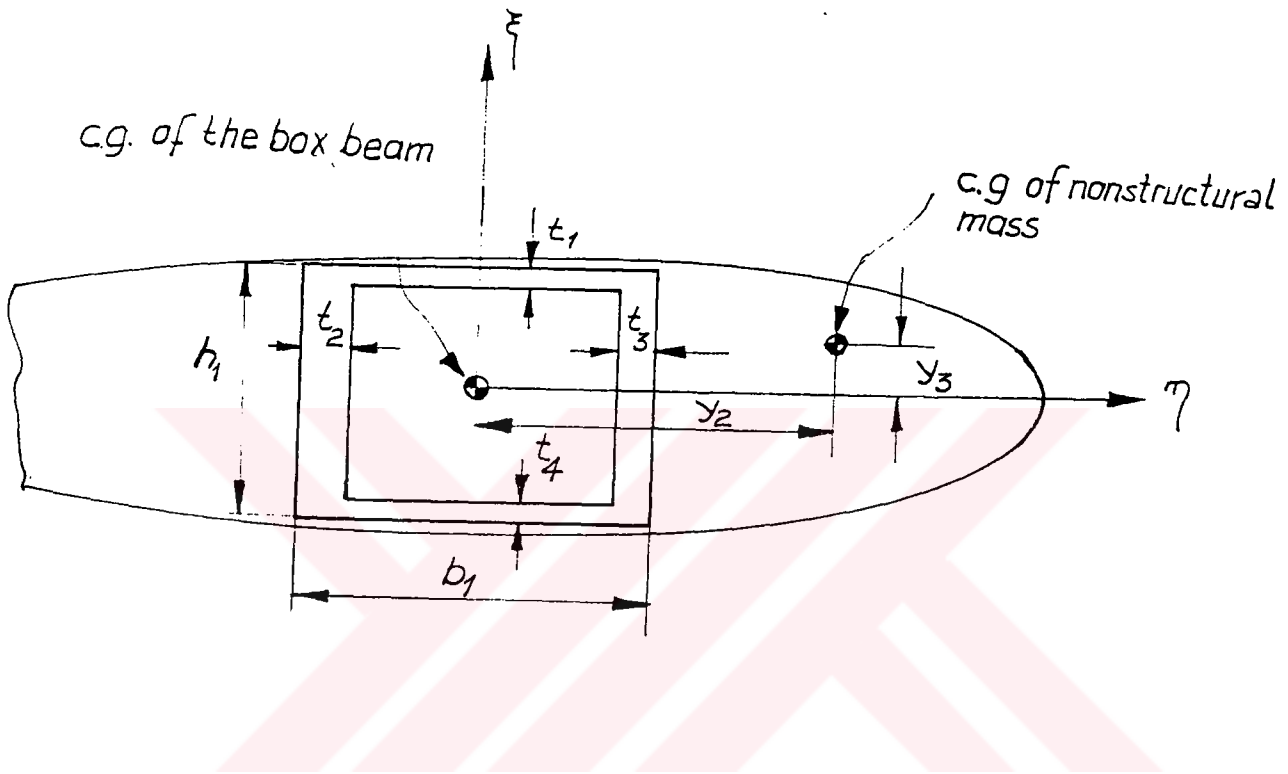


Figure 2.1: Box Beam Structure Geometry

discrete parameter form of the rotor blade equations are given by reference [44]. These equations are discretized by Galerkin type finite element method and are for general coupled flap-lag-torsion dynamics of a hingeless rotor blade both for forward and hover flight conditions with arbitrary mass and stiffness distributions. Cross sectional mass center and aerodynamic center offsets from the elastic axis are also included. Quasisteady aerodynamics has been used in developing the equations where the compressibility and stall effects are not included. The problem of weight minimization subject to a constraint on a natural frequency is often referred as to the dual problem. The primal problem is the one where the natural frequency is maximized holding the weight to a specified value. Both of these problems as applied

to optimum design of nonrotating beams with thin-walled cross sections undergoing coupled bending and torsional vibrations have been addressed by Hanagud and Chattopadhyay [23,24]. It has been observed that the optimum distributions differ largely with and without the coupling effects.

## 2.1 Discretization of the Equations of Motion Using the Galerkin Finite Element Method

The first step in solving the equations of motion is the discretization of the spatial dependence. This is accomplished through application of the Galerkin finite element method. Subsequently, modal analysis is used to reduce the number of discrete unknowns describing the problem.

The approximate global solution given by equation (2.1) is extended to include the torsional deformation:

$$\{q^g\} = \begin{Bmatrix} \bar{V}^g \\ \bar{W}^g \\ \phi^g \end{Bmatrix} = [\Phi_m] \{b_m\} \quad (2.1)$$

This solution is now substituted into the flap-lag-torsion equations of motion, Equation (B.2) and (B.4) and the corresponding boundary conditions. Recall, that in the extended Galerkin method the shape functions  $\phi_m$  need to satisfy only the geometric boundary conditions. Therefore, both the natural boundary conditions at the blade tip, Equations (B.6a-c), and the mixed boundary condition, due to the root torsional spring, Equation (B.5b), contribute to the boundary residual.

The weighted Galerkin residual, obtained through appropriate combination of the weighted differential equation and boundary condition residuals is given below.

$$\begin{aligned}
& \int_0^1 [\Phi_m]^T \left\langle \begin{aligned} & -\left(M_{3,x} + \bar{G} \bar{J} \phi_{,x} \bar{W}_{,xx} - \bar{V}_{,x} \bar{T}\right)_{,x} - q_{3l,x} \\ & \left(M_{2,x} + \bar{G} \bar{J} \phi_{,x} \bar{V}_{,xx} + \bar{W}_{,x} \bar{T}\right)_{,x} + q_{2l,x} \\ & M_{x,x} \end{aligned} \right\rangle^g \\
& + \left\langle \begin{aligned} & p_{yl} + p_{yA} + p_{yD} \\ & p_{zl} + p_{zA} + p_{zD} \\ & M_1 + q_{1l} + q_{xA} + q \end{aligned} \right\rangle d\bar{x}_0 \\
& + [\Phi_{m(l)}]^T \left\langle \begin{aligned} & \left(M_{3,x} \bar{G} \bar{J} \phi_{,x} \bar{W}_{,xx} - \bar{V}_{,x} \bar{T} + q_{3l}\right) - M_3 \\ & -\left(M_{2,x} + \bar{G} \bar{J} \phi_{,x} \bar{V}_{,xx} + \bar{W}_{,x} \bar{T} + q_{2l}\right) + M_2 \\ & -M_x \end{aligned} \right\rangle_{\bar{x}_0=1}^g \\
& + [\Phi_{m(0)}]^T \left\langle \begin{aligned} & 0 \\ & 0 \\ & M_x - \bar{K}_\phi \phi \end{aligned} \right\rangle_{\bar{x}_0=0}^g = 0 \quad (2.2)
\end{aligned}$$

Integrating by parts and cancelling the boundry terms, the final expression, corresp is obtained as :

$$\begin{aligned}
& \int_0^1 \left\langle [\Phi_m]^T \begin{Bmatrix} M_3 \\ -M_2 \\ 0 \end{Bmatrix} + [\Phi_m]^T \begin{Bmatrix} -\bar{G} \bar{J} \phi_{,x} \bar{W}_{,xx} + \bar{V}_{,x} \bar{T} - q_{3l} \\ \bar{G} \bar{J} \phi_{,x} \bar{V}_{,xx} + \bar{W}_{,x} \bar{T} + q_{2l} \\ M_x \end{Bmatrix} \right\rangle^g \\
& - [\Phi_m]^T \left\langle \begin{Bmatrix} p_{yl} + p_{yA} + p_{yD} \\ p_{zl} + p_{zA} + p_{zD} \\ M_1 + q_{1l} + q_{xA} + q_{xD} \end{Bmatrix} \right\rangle d\bar{x}_0 + [\Phi_{m(0)}]^T \left\langle \begin{Bmatrix} 0 \\ 0 \\ \bar{K}_\phi \phi \end{Bmatrix} \right\rangle_{\bar{x}_0=0}^g = 0 \quad (2.2)
\end{aligned}$$

In the interior of the element the displacements are given by:

$$\{q^g\} = \begin{Bmatrix} \bar{V}^g \\ \bar{W}^g \\ \phi^g \end{Bmatrix} = \begin{bmatrix} \gamma^T & 0 & 0 \\ 0 & \eta^T & 0 \\ 0 & 0 & \phi^T \end{bmatrix} \begin{Bmatrix} h^e \\ g^e \\ f^e \end{Bmatrix} = [\Psi(\bar{X}_e)] \{\alpha^e(\Psi)\} \quad (2.3)$$

For more information see Appendix A and Appendix B.

## 2.2 Formulation of Equality Frequency Constraints Problem

The discrete parameter form of the governing equation of the rotor blade motion is given by Reference [44] as

$$M\ddot{q} + (C + \hat{C})\dot{q} + (K + K_A)q = f(t) \quad (2.4)$$

in above equation,  $K = K_S + K_A$  is a real unsymmetric matrix where indices S and A corresponds to structural and aerodynamic effects respectively. Finite element used to discretize the blade and the associated degrees of freedom are shown in Figure 2.2. In this simplified analysis rotor blade motion in hover case is considered. The linear undamped motion of the rotor blade is given by

$$M\ddot{q} + (K_S + K_A)q = f(t) \quad (2.5)$$

Elemental degrees of freedom are rearranged such that,

$$q^e = \{v_1, v'_1, w_1, w'_1, \phi_1, v_2, v'_2, w_2, w'_2, \phi_2\}^T$$

The eigenvalue problem of the nonsymmetric system can be written as [45].

$$\begin{aligned} (K - \omega_i^2 M) q_i &= 0 \\ (K^T - \omega_i^2 M^T) s_i &= 0 \end{aligned} \quad (2.6)$$

where  $q_i$  and  $s_i$  are defined as right and left eigenvectors corresponding to the  $i$ th eigenvalue,  $\omega_i^2$ . Both sets of eigenvectors can be expressed as square matrices  $Q$  and  $S$  as

$$\begin{aligned} Q &= [q_1, q_2, \dots, q_n] \\ S &= [s_1, s_2, \dots, s_n] \end{aligned} \quad (2.7)$$

and orthonormality conditions can be also written as,

$$\begin{aligned} S^T M Q &= [I] \\ S^T K Q &= [\Lambda] \end{aligned} \quad (2.8)$$

where  $\Lambda$  is a diagonal matrix with eigenvalues on its diagonals.

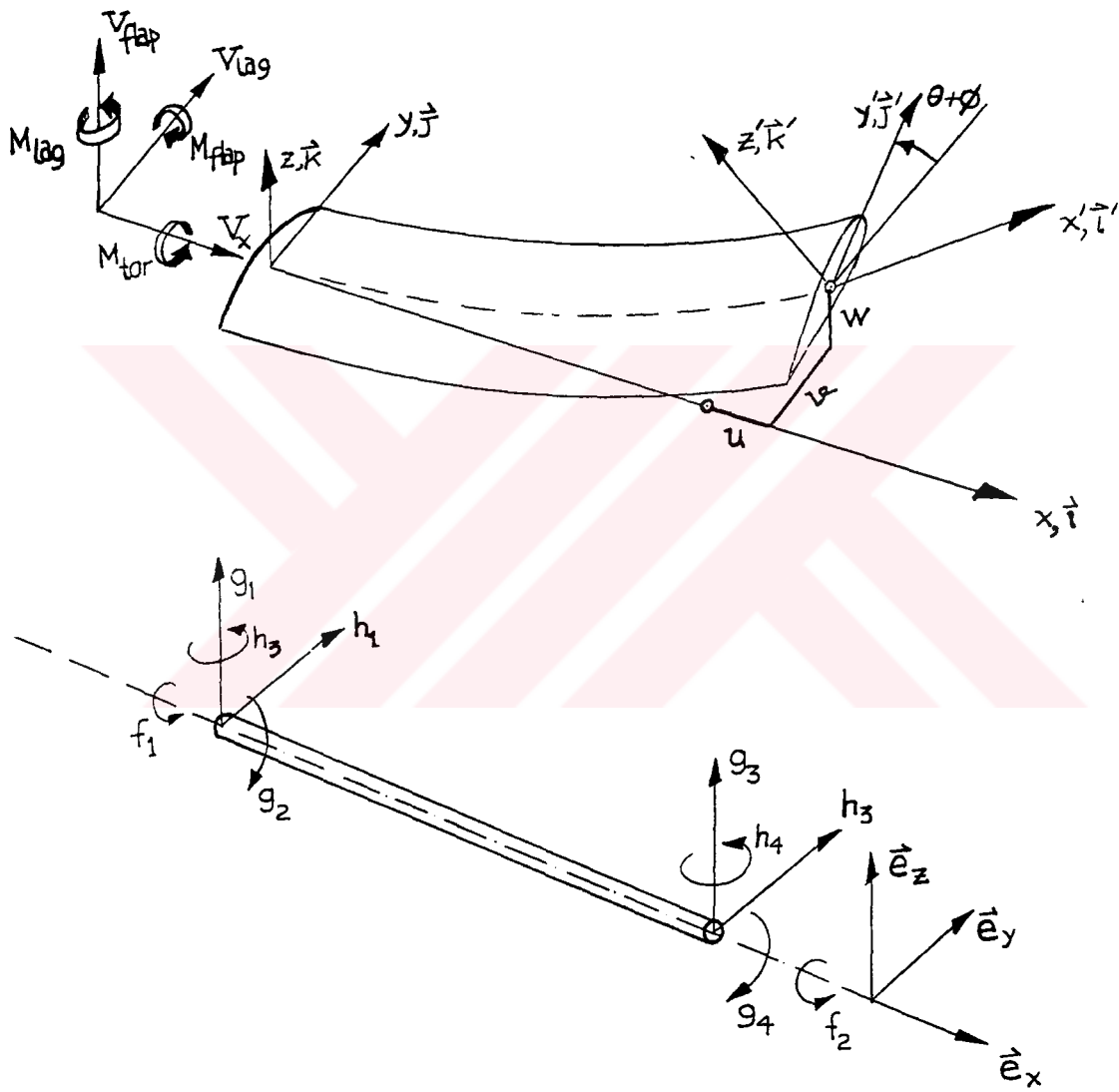


Figure 2.2: Beam Type Finite Element and the Associated Degrees of Freedom

### 2.2.1 Formulation of the Optimization Problem

The total weight of the resulting discretized blade is

$$W = \sum_{i=1}^{n_t} (\rho_{e_i} l_{e_i} A_{e_i} + W_{t_i}) \quad (2.9)$$

where,  $\rho_{e_i}$ , is the material density,  $l_{e_i}$  is the element length,  $A_{e_i}$  is cross sectional area and  $W_{t_i}$  is the nonstructural mass. The optimization problem can now be posed as follows:

Minimize:

$$W = \sum_{i=1}^n (\rho l A + W) \quad (2.10)$$

Subject to:

Equilibrium condition;

$$\begin{aligned} (K - \omega_k^2 M) q_k &= 0 \\ (K^T - \omega_k^2 M^T) s_k &= 0 \end{aligned} \quad (2.11)$$

Orthonormality condition;

$$\begin{aligned} s_k^T M q_l &= \delta_{kl} \\ s_k^T K q_l &= \delta_{kl} \omega_{kl} \end{aligned} \quad (2.12)$$

Besides design variables are bounded by lower and upper limits;



$$\phi_{\min} \leq \phi_n \leq \phi_{\max} \quad (2.13)$$

As a first step only the problem of unsymmetric matrices and the associated frequency constraints are considered. As the next step, the constrained optimization problem is now converted into an unconstrained one by the use of Lagrange multipliers. The modified objective function is written as

$$\begin{aligned} W^* = & \sum_{i=1}^n (\rho_{e_i} l_{e_i} A_{e_i} + W_{t_i}) \\ & - \mu_1 (s_k^T K_{e_i} q_k - \omega_k^2) - \mu_2 (q_k^T K_{e_i}^T s_k - \omega_k^2) \\ & - \nu_1 (s_k^T M_{e_i} q_k - 1) - \nu_2 (q_k^T M_{e_i}^T s_k - 1) \\ & - \Omega_1 (K_{e_i} - \omega_k^2 M_{e_i}) q_k - \Omega_2 (K_{e_i}^T - \omega_k^2 M_{e_i}^T) s_k \end{aligned} \quad (2.14)$$

In above equation  $\omega_k$  is the frequency which is desired to set equal to the  $\nu$ ,  $s_k$  and  $q_k$  are the corresponding eigenvectors of the rotor blade system. The problem now is to minimize  $W^*$  subject to the constraints on the design variables. The se constraints are given by equation 2.13. This is done by obtaining stationary value of the objective function  $W^*$  using full resources of variational techniques, While staying within the bounds on the design variables.

The necessary condition for the stainerity is given by,

$$\Delta W^* = 0 \quad (2.15)$$

This leads to the condition,

$$\frac{\partial W^*}{\partial q_1} = 0$$

$$\frac{\partial W^*}{\partial s_1} = 0 \quad (2.16)$$

In view of equation 1.3 and 1.9, these conditions yield to

$$\begin{aligned} \Omega_1 &= -(\mu_1 + \mu_2) s_1 \\ \Omega_2 &= -(\mu_1 + \mu_2) q_1 \end{aligned} \quad (2.17)$$

and

$$v_1 + v_2 = -\omega_i^2 (\mu_1 + \mu_2) \quad (2.18)$$

The next requirement is  $\frac{\partial w^*}{\partial \phi_i} = 0$  and can be derived from equation 2.14. This

follows a set of optimality criteria condition given below,

$$\begin{aligned} \frac{\partial W^*}{\partial \phi_n} &= \rho_{e_i} l_{e_i} \frac{\partial A_{e_i}}{\partial \phi_n} \\ &- \mu_1 \left( s_{k_i}^T \frac{\partial K_{e_i}}{\partial \phi_n} q_{k_i} \right) - \mu_2 \left( q_{k_i}^T \frac{\partial K_{e_i}^T}{\partial \phi_n} s_{k_i} \right) \\ &- v_1 \left( s_{k_i}^T \frac{\partial M_{e_i}}{\partial \phi_n} q_{k_i} \right) - v_2 \left( q_{k_i}^T \frac{\partial M_{e_i}^T}{\partial \phi_n} s_{k_i} \right) \\ &- \Omega_1^T \left( \frac{\partial K_{e_i}}{\partial \phi_n} - \omega_k^2 \frac{\partial M_{e_i}}{\partial \phi_n} \right) q_{k_i} - \Omega_2^T \left( \frac{\partial K_{e_i}^T}{\partial \phi_n} - \omega_k^2 \frac{\partial M_{e_i}^T}{\partial \phi_n} \right) s_{k_i} \end{aligned} \quad (2.19)$$

Using equations 2.17,2.18,2.19 the optimality condition is rewritten as

$$\frac{\partial A_{e_i}}{\partial \phi_n} \rho_{e_i} l_{e_i} - \mu \left( \omega_k^2 s_{k_i}^T \frac{\partial M_{e_i}}{\partial \phi_n} q_{k_i} - s_{k_i}^T \frac{\partial K_{e_i}}{\partial \phi_n} q_{k_i} \right) = 0 \quad i = 1, 2, \dots, n_i \quad (2.20)$$

where  $n_t$  denotes the number of elements over which the design variable  $\phi_i$  does not reach the limiting values posed by equation 2.13. Note that the global mass and stiffness matrices  $M$  and  $K$  are replaced by the corresponding elemental quantities  $M_{e_i}$  and  $K_{e_i}$  respectively,. Similary eigenvectors  $q_k$  and  $s_k$  are also replaced by corresponding elemental eigenvectors  $q_k$  and  $s_k$ . This has been done since there exist a one to one correspondence between an element and a design variable or in other words,  $\phi_n$ , only appears in the element stiffness and mass matrices of the  $i$ th element. A simultaneous solutions of equations 2.10, 2.11, 2.12, and equation 2.20 with in the bounds equation 2.13 will result in possible optimum designs.

### 2.2.2. Recursion Relations

The optimization procedure begins with a set of feasible initial values for the design variables. For this initial design, solutions of equations 2.11, and 2.12, will provide the eigenvalue  $\phi_n$  and the associated eigenvectors  $q_k$  and  $s_k$ . Next, it is necessary to solve for the Lagrange multiplier  $m$ . From equation 2.20, it is seen that there exists  $n_t$  equations involving a single unknown  $\mu$ . An exact solution of  $\mu$  is therefore not possible. In fact, only on rare occasions a solution of the optimality conditions provides immediate solutions of the Lagrange multipliers. Hence, an approach for finding an estimated or best value of the Lagrange multiplier, which will denoted by  $\bar{\mu}$ , is necessary. Once the value  $\bar{\mu}$  is obtained, it is necessary to obtain a set of recursive relations of redesign equations which will provide an updated set of values for the design variables. Based on these recursion relations, an iterative scheme is developed to move through the design space in such manner as the eventually locate a stationary design that statisfies the optimality criteria exactly and therefore is an optimum design. This is done as follows:

Denote:

$$A_i = s_{e_i}^T \frac{\partial M_{e_i}}{\partial \phi_{e_i}} q_{e_i}$$

$$B_i = s_{e_i}^T \frac{\partial K_{e_i}}{\partial \phi_{e_i}} q_{e_i} \quad (2.21)$$

The optimality criterion of equation 2.20 can now be written as

$$C_i - \mu(\omega_i^2 A_i - B_i) = 0 \quad i = 1, 2, \dots, n_t \quad (2.22)$$

By defining,

$$Z_i = \mu^2 A_i - B_i \quad (2.23)$$

equation 2.27 is written as

$$\frac{C_i}{\mu} - Z_i = 0 \quad i = 1, 2, \dots, n_t \quad (2.24)$$

At the optimum design, there exists a single value of  $\mu$  which will satisfy equation 2.24 exactly. However, for a non-optimum design since there is no such single value for  $\mu$ , an approach for finding a estimated value for  $\mu$  is derived. A least square type of approach has been used for this purpose. Since equations 2.24 are exactly satisfied for a unique value of  $\mu$  only at the optimum designs, a residual  $R_i$  is defined where

$$R_i = \frac{C_i}{\bar{\mu}} - Z_i \quad i = 1, 2, \dots, n_t \quad (2.25)$$

At the optimum design,  $R_i = 0$  for  $i = 1, 2, \dots, n_t$ . At nonoptimum designs it is necessary to make  $\bar{\mu}$  as close to the exact  $\mu$  as possible. Hence, the idea is to take

the sum of the squares of the residuals and minimize it with respect to  $\bar{\mu}$  Reference [24]. That is set,

$$\frac{d}{d\bar{\mu}} \left( \sum_{i=1}^{n_i} R_i^2 \right) = 0 \quad (2.26)$$

which gives at the (n+1) th iteration, the design process requires that

$$\bar{\mu} = \frac{\sum_{i=1}^{n_i} C_i^2}{\sum_{i=1}^{n_i} (\omega_i^2 A_i - B_i) C_i} = \frac{n_i C_i}{\sum_{i=1}^{n_i} (\omega_i^2 A_i - B_i)} \quad (2.27)$$

at the (n+1) th iteration, the design process requires that

$$\begin{aligned} B_i^{n+1} &= \omega^2 A_i^{n+1} - \frac{1}{\bar{\mu}^n} C_i^{n+1} & \bar{\mu}^n < 0 \\ \omega^2 A_i^{n+1} &= B_i^{n+1} + \frac{1}{\bar{\mu}^n} C_i^{n+1} & \bar{\mu}^n > 0 \end{aligned} \quad (2.28)$$

The above equations are written in such a manner as to ensure positive quantities on the either side of the equality sign and are necessary to develop the recursive relations. These relations are used to obtain improved value of the design variables and are presented below. The deatils can be found in Reference [24].

$$\begin{aligned} \phi_i^{n+1} &= \phi_i^n \left[ \left( \frac{\bar{\omega}}{\omega^n} \right)^\alpha \left\{ \frac{(\omega^2) A_i^n}{B_i^n + \frac{1}{\bar{\mu}} C_i^n} \right\}^\beta \right], & \bar{\mu}^n > 0 \\ \phi_i^{n+1} &= \phi_i^n \left[ \left( \frac{\bar{\omega}}{\omega^n} \right)^\alpha \left\{ \frac{B_i^n}{(\omega^n)^2 A_i^n - \frac{1}{\bar{\mu}} C_i^n} \right\}^\beta \right], & \bar{\mu}^n < 0 \end{aligned} \quad (2.29)$$

where  $\alpha$  is a positive exponent,  $\beta$  is a relaxation parameter,  $\bar{\omega}$  is the equality constraint of the desired frequency.

The rationale for using a scaling factor of  $\frac{\bar{\omega}}{\omega^n}$  in the recursive relations has been explained in Reference [39].

### 2.2.3 Convergence Criteria

Once a set of new values of design variables are obtained, the same convergence criteria as used in Reference [39] are used. They are

$$\Delta\omega = \frac{\bar{\omega} - \omega_i}{\bar{\omega}} < \epsilon_1 \quad (2.30)$$

$$\Delta W = \frac{\bar{W} - W^{n+1}}{W_{n+1}} < \epsilon_2 \quad (2.31)$$

where  $\epsilon_1$  and  $\epsilon_2$  are small prescribed tolerances,  $W$  is a weight obtained from a previous design that satisfies the condition given by equation 2.29 and  $W^{n+1}$  denotes the weight at the  $(n+1)$ th iteration. The iteration scheme used is the same as in Reference [39].

## CHAPTER 3

### RESULTS ARE DISCUSSION

#### 3.1.Configuration Definitions

In this section, numerical results are presented for selected soft and stiff inplane blade configurations under the condition of hover. The initial blade configuration, before the start of the optimization process it is assumed that blade had uniform cross sectional mass and stiffness distributions. Off-sets between the aerodynamic center with elastic center and mass centers are assumed to be equal to zero throughout the analysis.

For the numerical analysis, a typical hingeless rotor blade parameters are given in Table 3.1 are aimed to achieved. Structural loas carrying part of the blade is assumed to be a closed thin waaed box beam and made of aluminum. Cross section of this symmetric box beam is shown in Figure 2.1. Initial box beam dimensions are also listed in Table 3.2 where  $b_1$  chordwise dimension of the beam is choosen as the design variable for the optimization process. The rotor blade is devided into ten beam elements and the beam element and the associated degrees of freedoms are shown in Figure 2.2. In order to match the desired initial nondimensional chordwise stiffness values,  $b_1$  is choosen as 40 mm and 60 mm for soft and stiffinplane configurations respectively.

Mass per unit length of the rotor blade is consisted of the mass of the box beam,  $\rho A$ , and nonstructural mass,  $m_{ns}$ , of the blade the cross section.

$$m = \rho A + m_{ns}$$

where  $\rho$  is density,  $A$  is cross sectional area of the box beam and  $m_{ns}$  is the nonstructural blade cross sectional weight per unit lenngth of the blade excluding the box beam. Throughout the optimization process, the nonstructural blade mass is kept

as its initial design value and box beam cross-sectional weight is changed due to changes in the box beam geometry. Mass per unit length of the blade;

$$\bar{m} = \frac{m_{ns} + \rho A}{m_{AV}}$$

In view of mass per unit length definition. Nondimensional mass moment of inertias of the blade cross section are written as,

$$\bar{I}_{m_2} = \frac{\rho I_2 + y_2^2 m_{ns}}{(\rho A_V + m_{ns}) R^2} \quad (3.1)$$

$$\bar{I}_{m_3} = \frac{\rho I_3 + y_3^2 m_{ns}}{(\rho A_V + m_{ns}) R^2} \quad (3.2)$$

where  $A_V$  is average cross-sectional area of the box beam,  $R$  is the length of the blade,  $I_2$  and  $I_3$  are cross-sectional moment of inertias of the box beam in chordwise and flapwise directions respectively. Similarly,  $y_2$  and  $y_3$  are the distances between the c.g. of of the nonstructural mass and the cross-sectional c.g. of the blade in chordwise and flapwise directions respectively as shown in Figure 2.1.

The values of  $y_2$  and  $y_3$  are choosen and nonstructural mass per unit length,  $m_{ns}$ , is calculated such a way that the desired nondimensional inertial values, given in Table 3.1, are achieved for the initial configuration. During the optimization process,  $\bar{I}_{m_2}$  and  $\bar{I}_{m_3}$  are slightly changed due to the changes in the box beam structure. Inertial values given in Table 3.1.

Similarly the cross sectional bending and torsional stiffnesses are nondimensionalized as

$$E^{-1} I_2 = \frac{EI_2}{m R^4 \omega^2} = \frac{I_2}{\left[ A_V + \frac{m_{ns}}{\rho} \right]} \frac{E}{\rho R^4 \omega^2} \quad (3.3)$$



$$E^{-}I_3 = \frac{EI_3}{mR^4\omega^2} = \left[ A_v + \frac{m_{ns}}{\rho} \right] \frac{E}{\rho R^4\omega^2}$$

$$G^{-}J = \frac{J}{mR^4\omega^2} = \left[ A_v + \frac{m_{ns}}{\rho} \right] \frac{G}{\rho R^4\omega^2}$$

For the desired bending and torsion stiffnesses, given in Table 3.1, values of  $\bar{E}/\rho R^4\omega^2$  and  $G/\rho R^4\omega^2$  are calculated based on the system parameters. The general geometry of the box beam stucture is arranged such a way that the dimensional rigidities  $I_2, I_3$  and  $J$  and the nonstructural mass  $m_{ns}$  satisfy the desired nondimensional parameters given in Table 3.1. During the optimization process,  $I_2, I_3$  and  $J$  are changed significantly due to changes in the box beam geometry and  $A_v$  is averaged as

$$A_v = \frac{\sum_i^{n_e} A_i}{n_e}$$

where  $A_i$  is the cross-sectional area of the each blade section and  $n_e$  is the number of these blade sections. Based on this averaged cross-sectional area, nondimensional mass per unit length,  $\bar{m}_i$ , is calculated as,

$$\bar{m}_i = \frac{A_i + \frac{m_{ns}}{\rho}}{A_v + \frac{m_{ns}}{\rho}} \quad (3.4)$$

Table 3.1: Configuration Parameters for Flap-Lag-Torsion Motions in Hover

First rotating lag Frequency	$\omega_{L1} = 0.732$ (soft) ( $EI_2 = 0.01079$ )
	$\omega_{L1} = 1.417$ (stiff) ( $EI_2 = 0.14745$ )
First rotating flap Frequency	$\omega_{F1} = 1.125$ ( $EI_1 = 0.01079$ )
First rotating torsion Frequency	$\omega_{\phi 1} = 3.176$ ( $GJ = 0.00203$ )
	$I_m = 0.00625$
	$\left( \frac{I_{m2}}{I_{m3}} \right) = 0.0$
Semicord	$\frac{b}{R} = 0.0275$
Drag Coefficient	$C_{do} = 0.01$
Solidity Ratio	$\sigma = 0.07$
Lock Number	$\nu = 5.5$
2-D Lift curve slope	$a = 2\pi$
Weight Coefficient	$C_w = 0.005$
Aerodynamic center offset	$X_A = 0.0$
Percone angle	$\beta_P = 0.0$

For the optimization process described in the previous section, derivatives of  $I_{m_2}, I_{m_3}, \dots, \bar{G}J$  with respect to the design variable  $\phi_i$  are required. These derivatives,  $\frac{\partial \bar{I}_{m_2}}{\partial \phi_i}, \frac{\partial \bar{I}_{m_3}}{\partial \phi_i}, \dots, \frac{\partial \bar{G}J}{\partial \phi_i}$  are nondimensionalized by dividing these quantities by  $R$ , length of the blade.

### 3.2. Numerical Results For Selected Rotorblade Configurations

#### 3.2.1. Soft Inplane Hingeless Rotor Blade

The first of results are obtained for the soft inplane blade configuration. Where the nondimensional chordwise bending stiffness of the blade is  $\bar{EI}_2 = 0.01079$  for the uniform initial blade configuration. For the soft inplane blade configuration desired

nondimensional rotating lagging frequency of the blade is around  $\omega_{1_{LAG}} = 0.80$  and this value is set as the equality constraint for the smallest lagging dominant frequency. Physically, to achieve the minimum weight, the optimization process tends to yield to a final blade configuration with zero stiffness at the tip, where free end boundary conditions are enforced, and infinite value of stiffness at the root of the blade, where built-in boundary conditions are enforced. Computationally such a solution is not possible for a discrete parameter form of governing equations. On the other hand, such a solution is also does not have any practical application. For these reasons, upper and lower bounds are introduced to the problem.

Three different lower bounds for the design variable are studied. For the first case, the ratio of the initial value and the lower bound of the chordwise width of the box beam is set equal to  $1/8$ . For the next two cases these ratios are chosen as  $1/4$  and  $1/2$  respectively. No upper bound for the design variable is enforced for any of these cases. For the soft inplane, the initial ratio of the chordwise and flapwise dimensions of the box beam was  $8/5$  and this ratio is kept as same throughout the optimization process. In other words, the flapwise dimension of the box beam is changed as the chordwise dimension is changed with the initial ratio of  $8/5$ .

Result for the case where the ratio of the lower bound for the design variable was chosen as  $1/8$ . This chosen ratio lets the optimization program to increase the design variable to be reduced to  $1/8$  of its initial value. For the ratio of  $1/8$ , which is the allowed lowest ratio for the design variable, the highest mass reduction %19.9 is obtained. The initial and optimized distribution of the design variable, chordwise and directly proportioned flapwise dimensions of the box beam structure, and the stiffness distributions are presented Figure 3.1.a and 3.1.b. A significant distribution change for the nondimensional chordwise stiffness distribution is observed where the design variable is proportional with the chordwise stiffness with its third power.

The resultant hub forces and moments are another major concern for evaluating the optimization procedure and the choose of the objective function. The peak to peak value of these forces and moments are calculated by three method given in Appendix A of Reference [22]. In this study, since a new approach to develop an explicitly

formulated optimization procedure is aimed, only the trend in the change of these forces and moments are investigated. An overall optimization or qualitatively calculation of the resultant hub forces and moments in the nonrotating frame are not aimed. Therefore the results only show the effect of the mass reduction and the frequency placement on the isolated blade root reactions.

The nondimensional peak to peak values of the blade root forces for the initial and optimized configurations are showed in Figure 3.1.c and 3.1.d respectively. These forces are calculated for the hovering case with Lock number  $\nu = 5.5$  solidity ratio  $\sigma = 0.07$  and the collective pitch was set equal to  $\theta_c = 0.2$  for the all cases. An overall reduction in blade root reactions are observed and the highest reduction is attended for lagwise force with 18.45% decrease. The lowest reduction is obtained for the  $M_{lag}$ . As 5.21%.

For the second case the ratio of the initial and the minimum value for the design variable was set equal to 1/4. Since the lower bound of the design variable is set equal to a higher value, the achieved mass reduction is less than the first case where the lower bound was set to be equal to 1/8. Similarly the blade root forces and moments are reduced in general with same range observed as in the first case. Results for the design variable, the stiffness distributions, force and moment reductions are shown in Figures 3.2.a-3.2.d respectively.

Figure 3.3.a-3.3.d depict the results for the case where the lower bound of the design variable is set to its highest value compared with the first two cases. As expected the lowest mass reduction is obtained for this lower bound configuration where the blade optimization is most restrained from converging to its idealical solution.

The overall results are tabulated in Table 3.3. As seen from Table 3.3, more

Table 3.2 :Cross Sectional Properties of the Box Beam Structure

SOFT INPLANE		STIFF INPLANE
$t_1$	2.5 mm	2.5 mm
$t_2$	7.5 mm	7.5 mm
$t_3$	7.5 mm	7.5 mm
$h_1$	25 mm	25 mm
$b_1$	40 mm	60 mm

Table 3.3: Optimization Results for the Soft Inplane Configuration

Case	Design Var.	Mass Red. %	$F_{lag}$	$F_{flap}$	$M_{flap}$	$M_{lag}$	$\phi_{min} / \phi_{max}$
1	$b_{1ini} = 40$ mm	19.9	18.5	13.9	12.4	5.2	1/8
2	$b_{1ini} = 40$ mm	17.6	18.8	14.2	13.4	4.4	1/4
3	$b_{1ini} = 40$ mm	13.2	31.2	2.0	27.4	0.3	1/2

mass reduction for the blade mass is observed when lower ratios for the lower bound for the design variable is used. An overall reduction in blade root forces and moments are observed in general. Our focus of interest is the trend of these reductions with different mass reductions. As the reductions in the blade mass is increased lesser reductions in  $F_{flap}$  and  $M_{lag}$  are observed. On the other hand, reductions in  $F_{flap}$  and  $M_{lag}$  are increased parallell with the increase in reduction of the blade mass which was defined as the objective function for the problem.

### 3.2.2.Hingeless Rotor Blade

The second group of the results are obtained for the stiff inplane blade configuration where the first rotating lag frequency is  $\bar{\omega}_{lag} = 1.417$  which correspond to the nondimensional nonrotating frequency of  $EI_2 = .14745$ . For this case, the constraint for the first lagging frequency is set equal to  $\bar{\omega} = 1.16$ . For the stiff inplane configuration, both upper and lower bounds for the design variable is choosen as 1/12

and upper bound is also set just taht its ratio is 2/1. This bounds represent the case where the design variables are least constrained compared with the next two cases. As expected, the highest mass reduction is obtained as 13.0%. Significant reductions are also observed for the individual blade root forces and moments except the  $M_{lag}$ . Blade root forces and moments are again calculated for the same hovering configuration parameters used for the soft inplane configuration. The results are presented in Figures 3.4.a-3.4.d In the second considered case, the ratios of lower and upper bounds for the

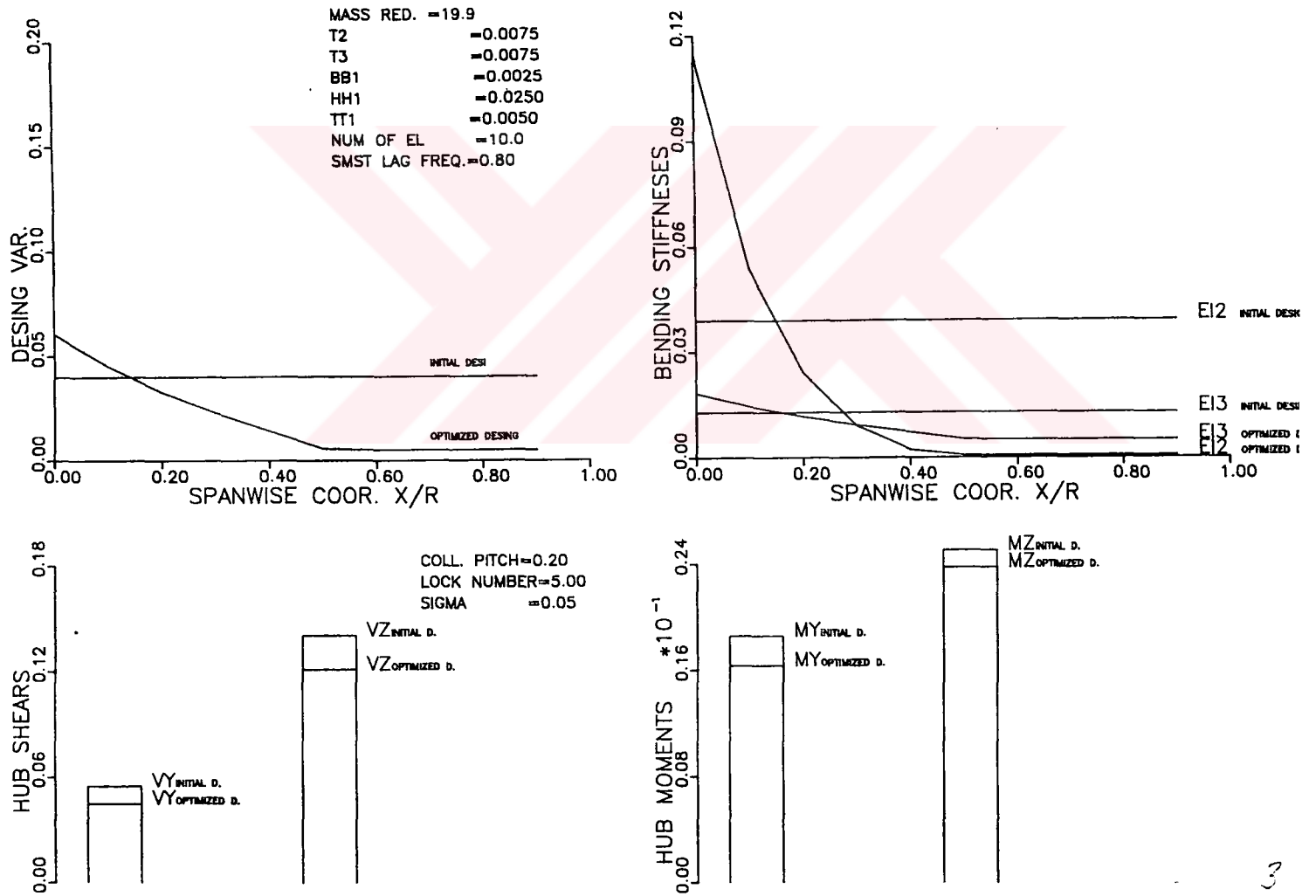


Figure 3.1: Results for Soft Inplane Configuration ,  $\phi_{min}/\phi_{ini} = 1/8$

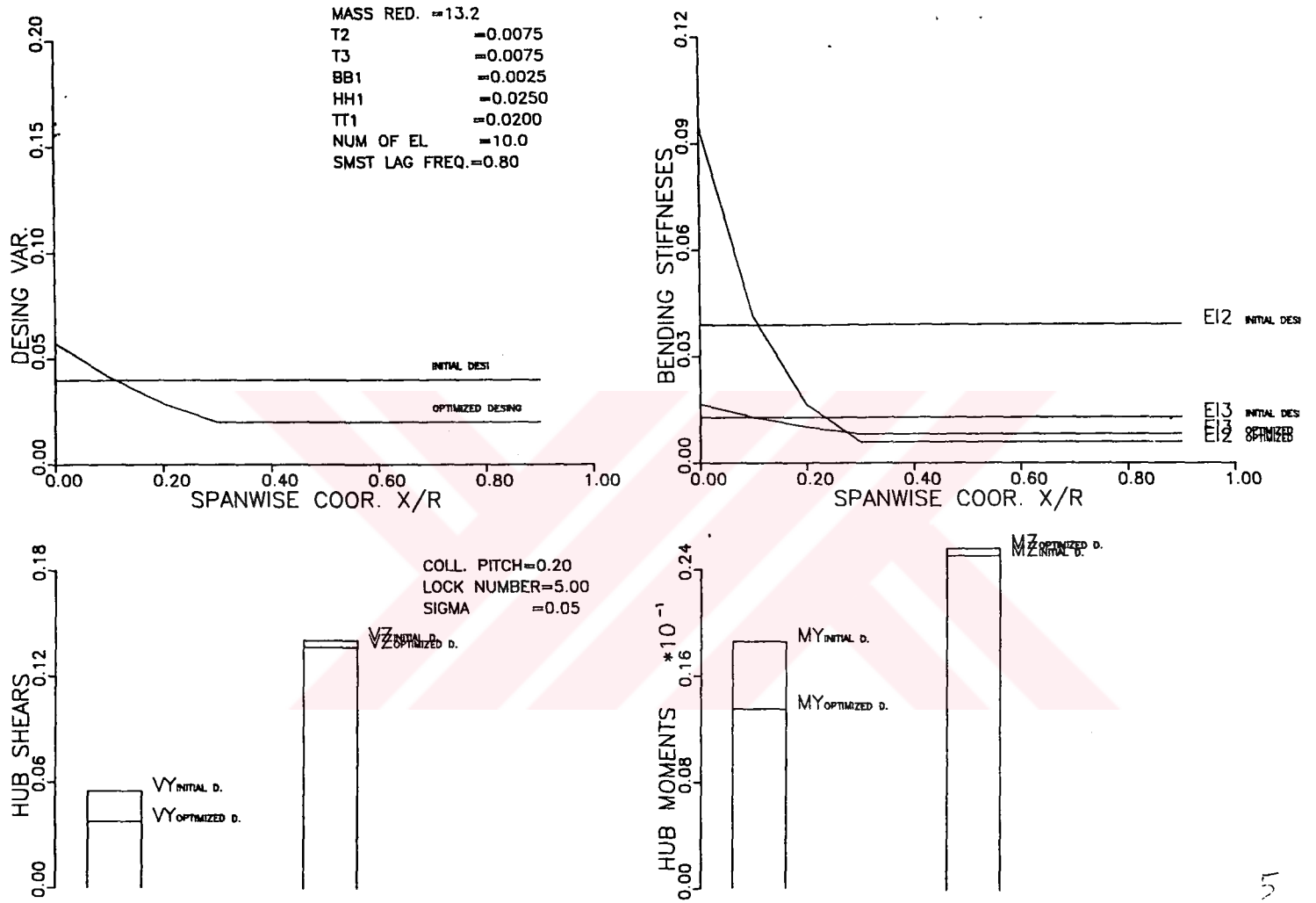


Figure 3.2: Results for Soft Inplane Configuration,  $\phi_{\min}/\phi_{ini} = 1/4$

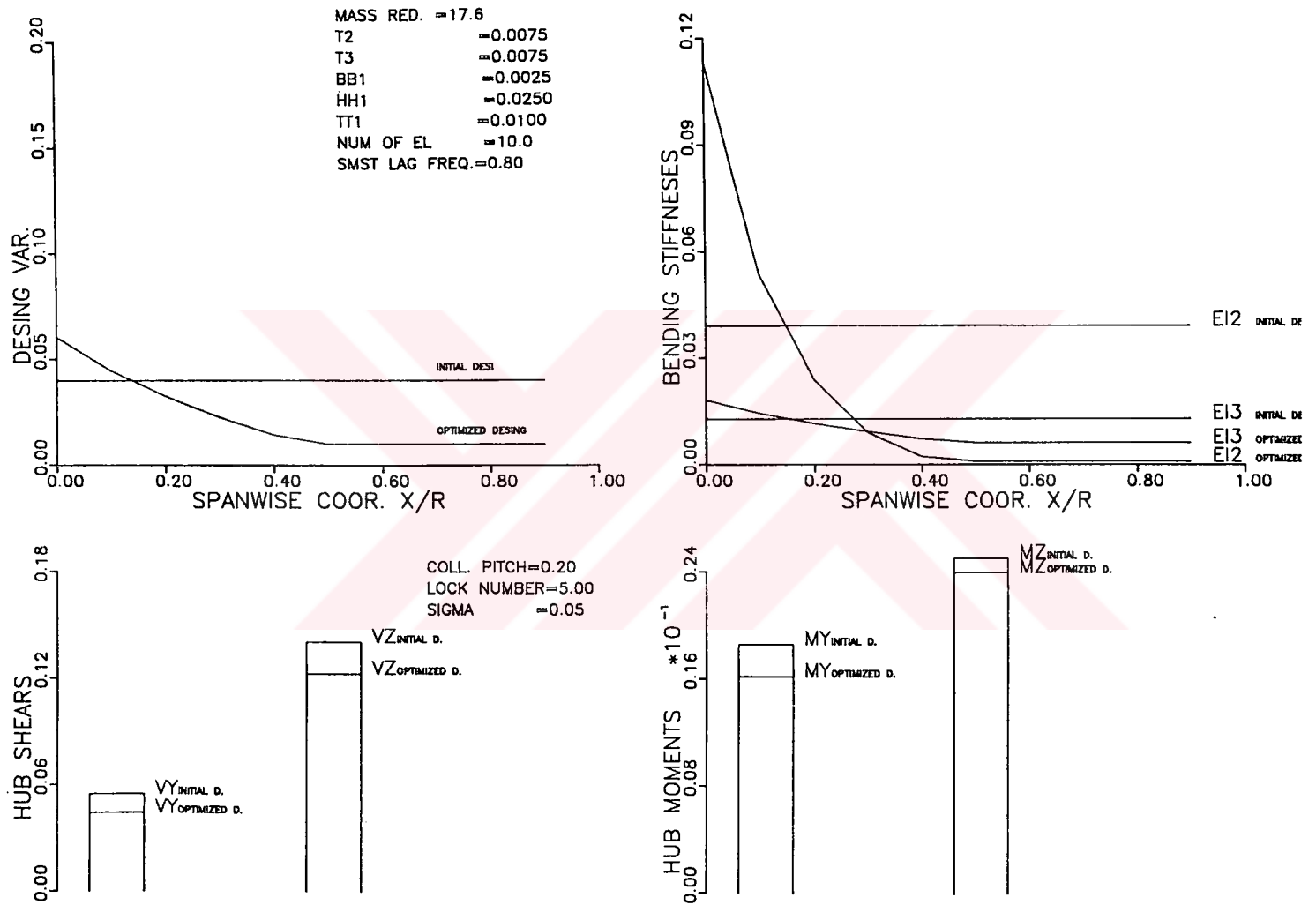


Figure 3.3 : Results for Soft Inplane Configuration,  $\phi_{\min}/\phi_{ini} = 1/2$



Table 4: Optimization Results For the Stiff Inplane Configuration

Case	Design Var.	Mass Red. %	$F_{lag}$	$F_{flap}$	$M_{flap}$	$M_{lag}$	$\phi_{min} / \phi_{max}$
1	$b_{l_{ini}} = 60 \text{ mm}$ $b_{l_{max}} = 125 \text{ mm}$	13	67.6	37.5	65.5	8.8	1/12
2	$b_{l_{ini}} = 60 \text{ mm}$ $b_{l_{max}} = 100 \text{ mm}$	7.6	70.3	35.8	68.8	9.4	1/3
3	$b_{l_{ini}} = 60 \text{ mm}$ $b_{l_{max}} = 90 \text{ mm}$	6.6	72.3	35.7	73.0	15.0	1/6

design variable are set as 1/3 and 5/3 respectively. These bounds represent a more restrictive case compared with the first considered case and as expected a lower mass reduction, 7.6% is obtained. Reductions in the forces and moments are in the same range of the first case. Figure 7.a-7.b show the results for this second case.

The last case considered for the stiff inplane configuration is the most restricted in terms of the upper and lower bounds on the design variable. The lower bound is chosen as 1/6 and the upper bound is set equal to 3/2. The lowest mass reduction is also observed for this configuration and only the 6.6 per cent of the blade mass is reduced. The similar trend in the reduction of the blade root reactions. Figures 8.a-8.d similarly depict the results for this case.

The overall results for the root reactions are tabulated in Table 4. Similar with the soft inplane case, the reactions increased, only  $F_{flap}$  and is increased but these changes was not significant compared with the changes in the reductions of other reactions. The reductions in the other reactions,  $F_{lag}$ ,  $M_{flap}$  and  $M_{lag}$  are decreased as the gains in the mass reductions are increased.

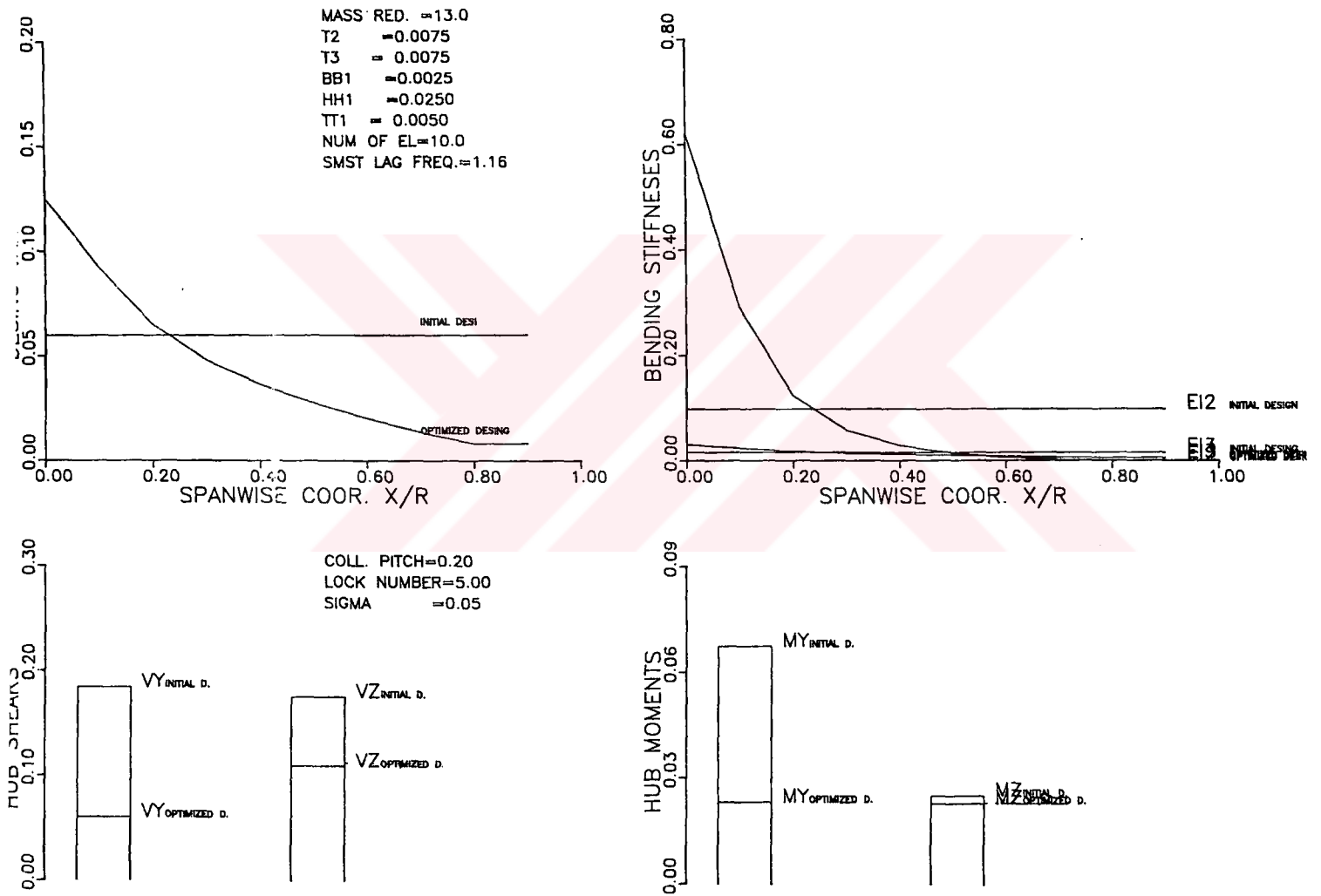


Figure 3.4: Results for Soft Inplane Configuration,  $\phi_{\min}/\phi_{ini} = 1/12$

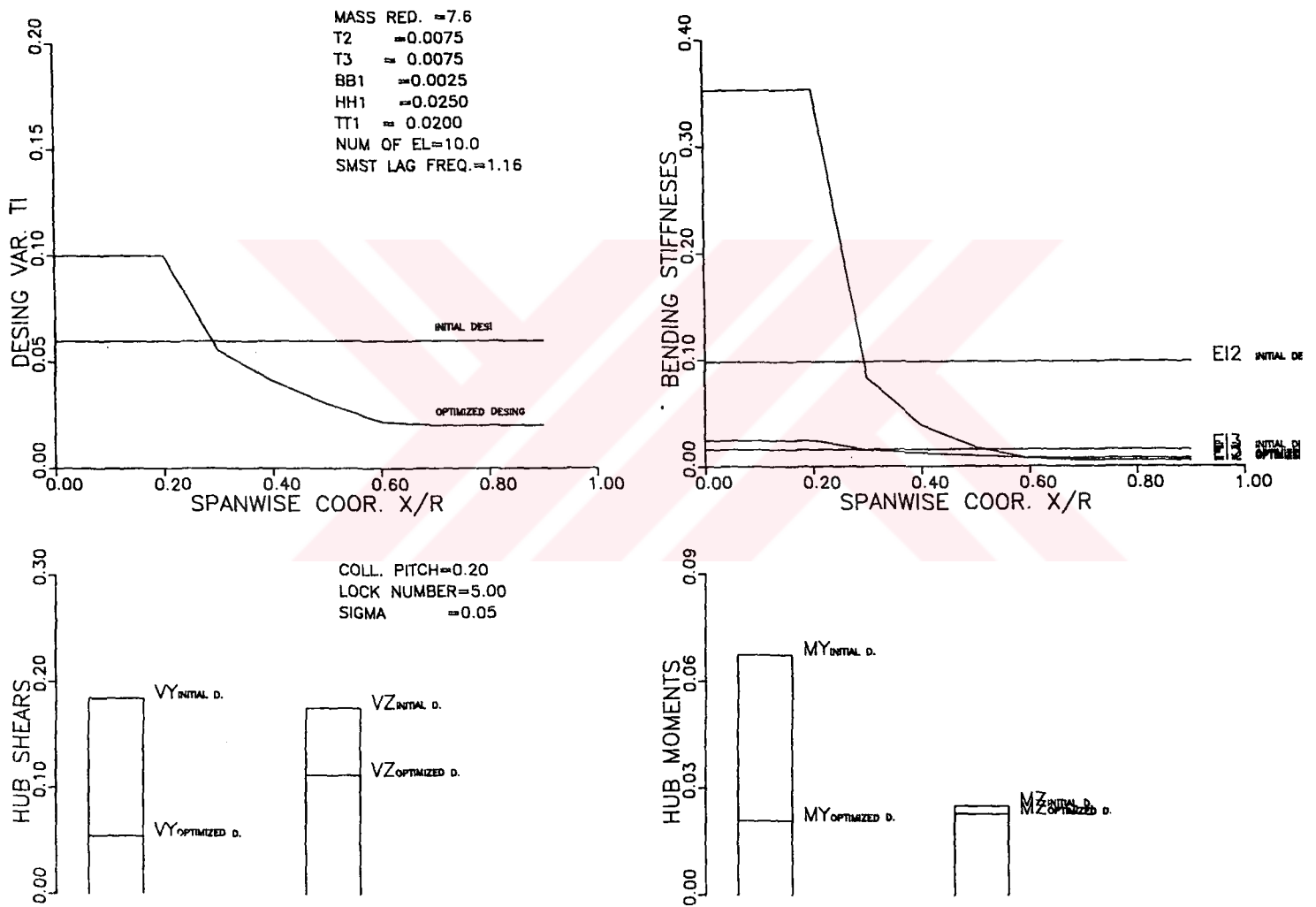


Figure 3.5 : Results for Soft Inplane Configuration,  $\frac{\phi_{\min}}{\phi_{ini}} = 1/3$

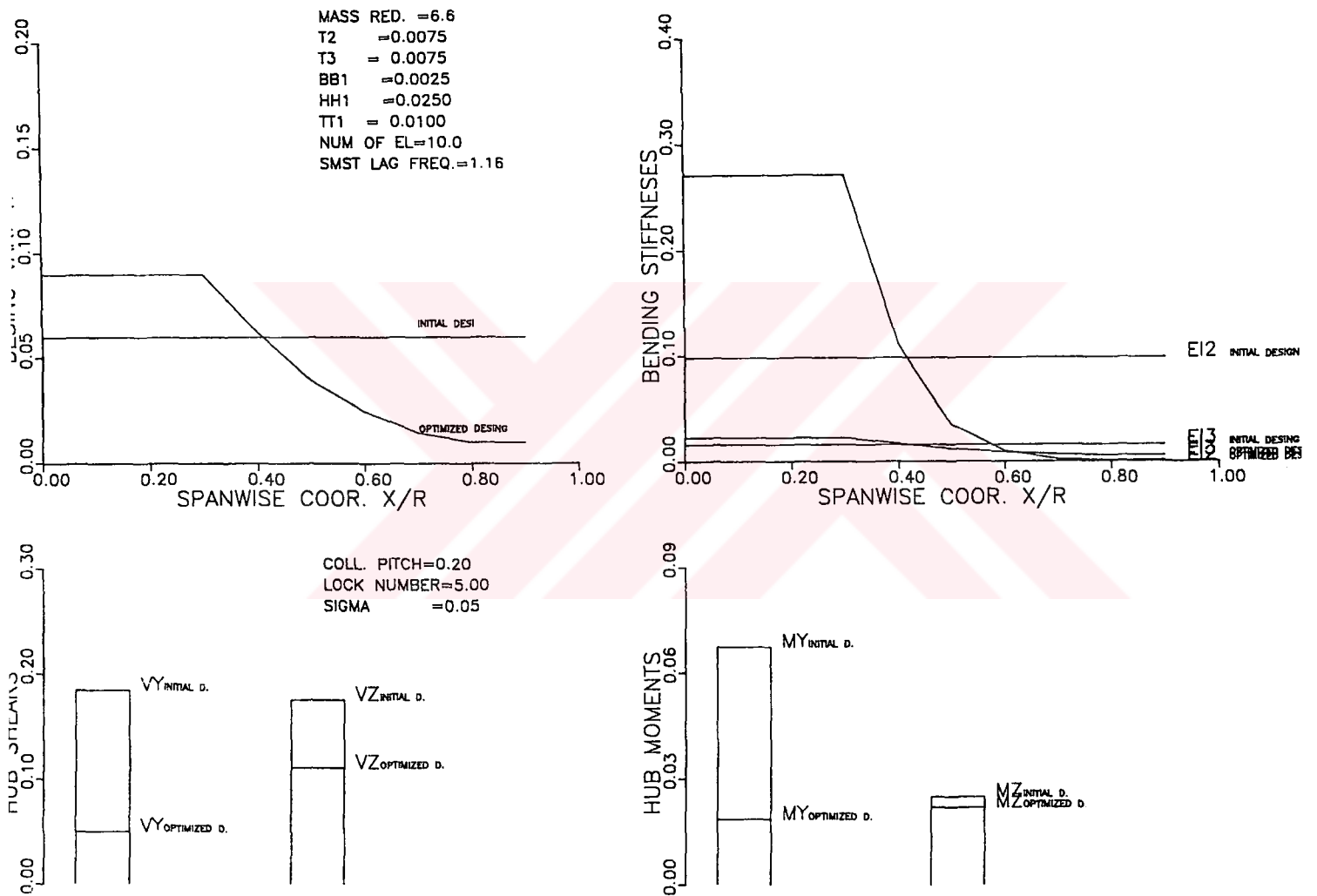


Figure 3.6: Results for Soft Inplane Configuration,  $\frac{\phi_{min}}{\phi_{ini}} = 1/6$

## REFERENCES

- [1] HIRSH, H., Dutton R.E., Rasumoff, A. "Effects of Spanwise and Chordwise Mass distribution on Rotor Blade Cyclic Stresses", Journal of American Helicopter Society, Vol.1, 1956
- [2] PETERS, D.A., Rossow, M.P., Korn, A., and Ko, T., "Design of Helicopter Rotor Blades for Optimum Dynamic Characteristics" Computers and Mathematical Applications, Vol.12A, June 1986
- [3] BIELEWA, R.L. "Techniques for Stability Analysis and Design Optimization with Dynamic Constraints of Nonconservative Linear Systems," AIAA/ASME 12<sup>th</sup> Structures, Structural Dynamics and Materials Conference, Anaheim, April 19-21, 1971
- [4] BENNETT, R.L., "Optimum Structural Design, " Proc. of the 38th Annual Forum of the American Helicopter Society, May 4-7, 1982
- [5] BENNETT, R.L., "Application of Optimum Design Techniques to Helicopter Design Problems," Report prepared by Bell Helicopter Textron, Inc., Under Contract NAS2-11666
- [6] FRIEDMANN, P.P., "Application of Modern Structural Optimization Methods to Rotor Design Problems," Vertica, Vol.7, 1983
- [7] FRIEDMANN, P.P., SHANTHAKUMARAN, P., "Optimum Design of Rotor Blades for Vibration Reduction in Forward Flight, " Journal of the American Helicopter Society, Oct. 1984
- [8] WALSH, J.L., BINGHAM, G.J., and RILEY, M.F., "Optimization Methods Applied to the Aerodynamic Design of Helicopter Rotor Blades, " Journal of the American Helicopter Society, Oct. 1985

- [9] TAYLOR, R.B., "Helicopter Vibration Reduction by Rotor Blade Modal Shaping," Proceedings of the 38th Annual Forum of the American Helicopter Society, May 4-7, 1982
- [10] BENNETT, R.L., "Application of Optimization Methods for Rotor Design Problems," Vertica, 1983
- [11] LIM, J.W., and CHOPRA, I., "Aeroelastic Optimization of A Helicopter Rotor," Journal of the American Helicopter Society, Jan. 1989
- [12] BANERJEE, D. and SHANTHAKUMARAN, P., "Application of Numerical Optimization Methods in Helicopter Industry," Vertica, 1989
- [13] HICKS, R.M., VANDERPLAATS, G.N., MURMAN, E.M., and KING, R.R. "Airfoil Section Drag Reduction at Transonic Speeds by Numerical Optimization," Paper No. 76-0477, Presented at the ASE Business Aircraft Meeting, Wichita, Kansas, April 6-7, 1976
- [14] TAUBER, M.E., "Computerized Aerodynamic Design of Transonic Rotor Blade" 40th Annual Forum of the American Helicopter Society, Crystal City, Virginia, May 16-18, 1984
- [15] HEAD, R.E. et al, "Design of McDonnell Douglas Helicopter Company Advanced Composite Rotor System," Proceedings of the 42th Annual Forum of the American Helicopter Society, Washington D.C., May 1986
- [16] CELL, R. and FRIEDMAN, P.P., "Structural Optimization with Aeroelastic Constraints of Rotor Blades with Straight and Swept Tips," 29th AIAA SDM Conference, Williamsburg, Virginia, April 1988
- [17] CHATTOPADHYAY, A. and WALSH, J.L., "Minimum Weight Design of Helicopter Rotor Blades with Frequency Constraints," Journal of the American Helicopter Society, Vol. 34, (4), Oct. 1989.

- [18] CHATTOPADHYAY, A. and WALSH, J.L., "Minimum Weight Design of Rectangular and Tapered Helicopter Rotor Blade with Frequency Constraints", NASA TM-100561, Feb. 1988
- [19] MARK, W.D., and WILLIAM, H.W., "Application of Design Optimization Techniques to Rotor Dynamics Problems," Journal of the American Helicopter Society, Vol. 33 (3), July 1988
- [20] MIURA, H., "Application of Numerical Optimization Methods to Helicopter Design Problems," Vertica, Vol. 9 (2), 1985
- [21] MIURA, H., "Application of Numerical Optimization Methods to Helicopter Design Problems; A Survey," NASA-TM 86010, Oct. 1984
- [22] HANAGUD, S., CHATTOPADHYAY, A., YILLIKÇI, Y.K., SCHRAGE, D., and REICHERT, G., "Optimum Design of a Helicopter Rotor Blade," 12th European Rotorcraft Forum, Garmish-Partenkirchen, West Germany, Sept. 22-25, 1986
- [23] HANAGUD, S., CHATTOPADHYAY, A., and SMITH, C.V., "Optimal Design of Vibrating Beam with Coupled Bending and Torsion," Proceedings of the 27th Annual Structures, Structural Dynamics and Material Conference, April 1985
- [24] HANAGUD, S., CHATTOPADHYAY, A., and SMITH, C.V., "Minimum Weight Design of a Structure with Dynamic Constraints and a Coupling of Bending and Torsion," Proceedings of the 28th Annual Structures, Structural Dynamics and Material Conference, San Antonio, Texas, May 1986
- [25] NIORDSON, F.I., "On the Optimal Design of Vibrating Beams," Quarterly of Applied Mathematics, Vol. 23., No. 1, 1965, pp. 47-63
- [26] BRANCH, R.M., "On the External Fundamental Frequencies of Vibrating Beams," International Journal of Solids and Structures, Vol. 4, 1968, pp. 667-674
- [27] VEPA, K., "On the Existence of Solutions of Optimization Problems with Eigenvalue Constraints," Quarterly of Applied Mathematics, Vol. 31, 1973-1974

[28] PRAGER, W., and TAYLOR, J.E. "Problems of Optimal Structural Design," Journal of Applied Mathematics, Vol.35, No.1, 1968

[29] TAYLOR, J.E., "Optimum Design of a Vibrating Bar with Specified Minimum Cross-Section," AIAA JOURNAL, Vol.5, No.7, July, 1968, pp. 1379-1381

[30] KAMAT, M.P., and SIMITSES, G.J., "Optimal Beam Frequencies by the Finite Element Displacement Method," International Journal of Solids and Structures, Vol.19, 1973

[31] KARIHALOO, B.L., and NIORDSON, F.I., "Optimum Design of Vibrating Cantilevers," Journal of Optimization Theory and Applications. Vol.4, No.6, 1973

[32] OLHOFF, N., "Optimization of Vibrating Beams with Respect to Higher Order Natural Frequencies," Journal of Structural Mechanics, Vol.5, No.2, 1977

[33] OLHOFF, N., "Maximizing Higher Order Eigen Frequencies of Beams with Constraints on the Design Geometry," Journal of Structural Mechanics Vol.5, No.2, 1977

[34] OLHOFF, N., "Optimization of Transversely Vibrating Beams and Rotating Shafts," Optimization of Distributed Parameter Structures," Sijthoff and Noordhoff, Alphen aan den Rijn, Netherlands, 1980

[35] TURNER, M.J., "Design of Minimum Mass Structures with Specified Natural Frequencies," AIAA Journal, Vol.5, No.3, March, 1967

[36] BRANCH, R.M., "On the Optimum Design of Vibrating Structures," Journal of Optimization Theory and Applications, Vol.11, No.6, 1973

[37] MCCAANT, B.R., HAUG, E.J., and STREETER, T.D., "Optimal Design of Structures with Constraints on Natural Frequency," AIAA Journal, Vol.8, 1970

[38] SIPPEL, D.L., and WARNER, W.H., "Minimum Mass Design of Multielement Structures with Constraints on Natural Frequency Constraint," AIAA Journal, Vol.11 April 1973



- [39] KHAN,M.R., and WILLMERT, K.D., "An Efficient Optimality Criterion Method for Natural Frequency Constrained Structures," Computers and Structures, 1981
- [40] VENKAYYA,V.B., and TISCHLER, V.A., "Optimization of Structures with Dynamic Constraints," Computer Methods for Nonlinear Solids and Structural Mechanics, Vol.54, Presented at the Applied Mechanics, Bioengineering and Fluids Engineering Conference, June 20-22, 1983
- [41] WARNER, W.H., and VAVRIK, D.J., "Optimal Design in Axial Motion for Several Frequency Constraints," Journal of Optimization Theory and Applications, Vol.15, 1975
- [42] PEDERSON, P., "Design with Several Eigenvalue Constraints by Finite Elements and Linear Programing," Journal of Structural Mechanics, Vol.10, 1982-1983
- [43] KNOT, N.S., "Optimization of Structures with Multiple Frequency Constraints," AFWAL-TI-83-29-FIBR-201, Wright-Patterson Air Force Base, Ohio, 1983
- [44] STRAUB, F.K., and FRIEDMANN, P.P., "Application of the Finite Element Method to Rotary Wing Aeroelasticity, NACA CR-165854, 1982
- [45] MEIROVITCH, L., "Computational Methods In Structural Dynamics," Sijthoff & Noor-hoof, Ntherlands, 1980
- [46] STRAUB,F.K.; 'Application of the Finite Element Method to Rotary-wing Aeroelasticity', Ph. D. Dissertation. School of Engineering and Applical Science, University of California, Los Angeles, 1980.

## APPENDIX\_A

### A.1.GALERKIN FINITE ELEMENT METHOD

From the preceding literature review it is evident that the Galerkin finite element method (GFEM) has been used successfully in treating a large number of nonself-adjoint and nonlinear problems. In the next section a brief description of the method will be given. Emphasis is placed on its application to nonself-adjoint systems. The GFEM, being applied directly to the governing differential equations, makes discretization of nonlinear terms straightforward. The ensuing nonlinear equations can then be solved with any of the algorithms used in the conventional finite element method.

#### A.1.1 Global Galerkin Method

The local Galerkin method, resulting in a finite element discretization, can best be clarified by illustrating its application to a simple system in References (8) and (11).

Consider the following differential equation

$$Q(q) + P(q) = F \quad (A.1)$$

which is defined in a domain  $D$ , where  $Q$  is a symmetric positive definite differential operator of order  $2r$  and  $P$  is a general operator of order  $r$  or less, representing the nonself-adjoint portion of equation. Both are operating on an unknown function  $q$  to yield a given function  $F$ . Furthermore, the function  $q$  has to satisfy certain boundary conditions on the boundary  $S$  of the domain  $D$ . For simplicity,  $q$  is chosen as a scalar function; however, the subsequent development is equally applicable to vector functions.

Next, an approximate global solution having the form,

$$q^s = \sum_{m=1}^M \phi_m b_m \quad (\text{A.2})$$

is assumed. The  $\phi_m$  are linearly independent shape functions and the  $b_m$  are the undetermined parameters for this problem. When using the extended Galerkin method,  $b_m$  have to have continuous derivatives up to order  $(r-1)$ , i.e.,  $C_{r-1}$  continuity. Further, they need to satisfy only the geometric boundary conditions, i.e., those containing derivatives of order not higher than  $(r-1)$ . This approximate solution is then substituted into the differential equation and the boundary conditions. The error is minimized by requiring orthogonality with respect to a set of weighting functions. Thus, an integral statement, equivalent to the differential equation and the boundary conditions, is obtained.

In the extended Galerkin method the original shape functions  $\phi_m$  are chosen as weighting functions. It is then required that the sum of the weighted residuals of both the differential equation and the natural boundary conditions, i.e., those containing derivatives of order  $r$  and higher, be zero (10). Thus,

$$\int_D \phi_m \epsilon_D dD + \int_S \phi_m \epsilon_B dS = 0 \quad m=1,2,\dots,M, \quad (\text{A.3})$$

where

$$\epsilon = Q(q^s) + P(q^s) - F \quad (\text{A.4})$$

and  $\epsilon_B$  is the residual associated with the natural boundary conditions.

In many cases it is possible to apply integration by parts to Eq. (A.3). This reduces the order of differentiation in the symmetric operator  $Q$ , thus lowering requirements on the shape functions  $\phi_m$  from  $C_{2r-1}$  to  $C_{r-1}$  continuity. Furthermore, this algebraic step also yields terms which cancel some of the boundary residual contributions. As a matter of fact, formulation of the weighted boundary residual are made in such a way

that, when integrating the last one by parts, identical terms of the boundry conditions are homogeneous, all boundary residual terms cancel out and Eq. ( A.3 ) becomes

$$\int_D \{ \overline{Q}(\phi_m, q^g) + \phi_m P(q^g) - \phi_m F \} dD = 0 \quad (A.5)$$

where  $\overline{Q}$  denotes the operator  $Q$  after integration by parts.

Application of the extended Galerkin method to beam bending can be found in Reference (51)

### A.1.2 Finite Element Approach

When formulating a finite element version of Galerkin's method the domain  $D$  is subdivided into  $E$  subdomains  $d$ , which are called elements. In each element an approximate solution of the form

$$q^e = \sum_{n=1}^N \psi_n^e \alpha_n^e \quad (A.6)$$

is assumed, where  $\alpha_n^e$  are the nodal parameters and  $\psi_n^e$  are linearly independent shape functions defined only in the subdomain associated with the element  $d$ . This local approximation can be extended over the whole domain  $D$  by defining

$$\xi_n^e = \begin{cases} \psi_n^e & \text{inside } d \\ 0 & \text{outside } d \end{cases} \quad (A.7)$$

Using Eq. ( A.7 ), the global approximation can be expressed as

$$q^g = \sum_{e=1}^E \sum_{n=1}^N \xi_n^e \alpha_n^e \quad (A.8)$$

After imposing compatibility conditions on the nodal parameters of adjacent elements (this is done during the process of assembly), equations (A.2) and (A.8) are equivalent.

Equation (A.5) can be rewritten using Eq. (A.8) as

$$\sum_{i=1}^E \sum_{n=1}^N \int_D \{ \bar{Q}(\xi_j^e, \xi_n^i) + \xi_j^e P(\xi_n^i) \} \alpha_n^i - \xi_j^e F \} = 0 \quad , \quad (A.9)$$

where  $\bar{Q}$  is obtained from  $Q$  by means of previously mentioned integration by parts. In addition, it is implicitly assumed that no inter-element discontinuities occur. Thus, the functions  $\xi_n^e$  and its derivatives of order  $r$  up to  $(2r-1)$  represents an intermediate step and in reality only Eq. (A.10) below is used.

As a consequence of the linear independence of the  $\xi_n^e$  functions, Equation (A.9) can also be rewritten on the element level.

$$\sum_{n=1}^N \int_d \{ \bar{Q}(\psi_j^e, \psi_n^e) + \psi_j^e P(\psi_n^e) \} \alpha_n^e - \psi_j^e F \} = 0 \quad (A.10)$$

$J=1,2,\dots,N, \quad e=1,2,\dots,E$

Equation (A.10) thus represents a set of  $N$  equations for each element, from which the element matrices can be calculated.

Because of the unique choice of weighting functions in Galerkin's method and because of the integration by parts,  $\bar{Q}$  yields symmetric matrices. Further, when  $P$  is equal to zero, Eq. (A.10) is the exact same expression as found when employing the variational formulation of the finite element method. Operator  $P$  leads to unsymmetric matrices. However, the banded nature of the system matrices is still preserved.

Assembly of the system matrices and enforcement of the geometric boundary conditions is handled as in the conventional finite element method.

Finally, it should be pointed out that when Equation ( A.3 ) is solved directly, the approximate solution has to have  $C_{2r-1}$  continuity and must satisfy all boundary conditions. The generation of such finite elements is of course more difficult, in particular for nonlinear terms, than generation of elements for the solution of Equation ( A.5 ). In addition, all matrices will be nonsymmetric. On the other hand, due to the higher-order continuity, one might expect more rapid convergence. Thus, it becomes obvious that integration by parts plays an important role.

### A.1.3 Convergence Properties

The Galerkin finite element method is equivalent to the conventional finite element method when considering self-adjoint problems. It is well known that elements which are conforming and are able to approximate constant strain will ensure convergence for this class of problems. Some elements even display monotonic convergence, thus allowing use of efficient extrapolation procedures and give an upper bound on the potential energy.

Based on Mikhlin's work (52),(53), Hutton and Anderson (11) and Kikuchi (9) established convergence criteria for the Galerkin finite element method when applied to a wider class of problems than those amenable to the variational FEM. However, numerical results show that convergence is, in general, not monotonic (22) and becomes less rapid when the nonself-adjoint character of the system under consideration becomes more pronounced (9).

Convergence studies for the Galerkin finite element method, when applied to nonlinear systems, are of numerical nature only (48).

Noor and Whiteman (54) derived an error bound for a certain class of nonlinear problems, solvable by the GFEM. There are a number of studies on convergence, accuracy, and stability of the FEM in nonlinear problems. They are, however, either

too general to be useful for practical applications or restricted to certain special classes of problems. On the other hand, a large number of nonlinear problems have been solved using the FEM with great success.

The comments made in this section are basically to be understood as an indication of the ongoing research effort. The rotary-wing aeroelastic problem because of its complexity will hardly be accessible to any convergence proof. Thus, for the time being, convergence can only be established numerically (55), i.e., by refining the discretization process.



## APPENDIX\_B

### APPLICATION OF THE METHOD TO THE FLAP-LAG-TORSION AEROELASTIC PROBLEM IN FORWARD FLIGHT

#### B.1 Brief Description of the Equations of Motion

The equation of motion for the flap-lag-torsion problem in forward flight are coupled nonlinear, nonconservative, partial differential equations with periodic coefficients. The structural operator is taken from Reference [56]. The inertia and aerodynamic loads are taken from Reference [2].

Axial equilibrium:

$$\bar{T}_{,x} + p_{xt} = 0 \quad (\text{B.1})$$

Lag equilibrium:

$$\begin{aligned} & -\left(M_{3,x} + \bar{G}\bar{J}\phi_{,x}\bar{W}_{,xx} - \bar{V}_{,x}\bar{T}\right)_{,x} \\ & -q_{3l,x} + P_{yt} + P_{yA} + P_{yD} = 0 \end{aligned} \quad (\text{B.2})$$

Flapequilibrium:

$$\begin{aligned} & \left(M_{2,x} + \bar{G}\bar{J}\phi_{,x}\bar{V}_{,xx} - \bar{W}_{,x}\bar{T}\right)_{,x} \\ & -q_{2l,x} + P_{zt} + P_{zA} + P_{zD} = 0 \end{aligned} \quad (\text{B.3})$$



Torsion equilibrium:

$$M_{x,x} + M_I + q_{II} + q_{xA} + q_{xD} = 0 \quad (\text{B.4})$$

The corresponding boundry conditions are :

At  $\bar{x}_0 = 0$ :

$$\bar{V} = \bar{W} = \bar{V}_{,x} = \bar{W}_{,x} = 0 \quad (\text{B.5a})$$

$$M_x - \bar{K}_\phi = 0 \quad (\text{B.5b})$$

At  $\bar{x}_0 = 1$ :

$$M_{3,x} - \bar{GJ}\phi_{,x}\bar{W}_{,xx} + \bar{V}_{,x}\bar{T} - q_{3I} = 0 \quad (\text{B.6a})$$

$$M_{2,x} + \bar{GJ}\phi_{,x}\bar{V}_{,xx} + \bar{W}_{,x}\bar{T} + q_{2I} = 0 \quad (\text{B.6b})$$

$$M_3 = -M_2 = M_x = 0 \quad (\text{B.6c})$$

$$\bar{T} = 0 \quad (\text{B.6d})$$

The boundry conditions at the free end,  $\bar{x}_0 = 1$ , are naturel boundry conditions, expressing the fact that the shears, moments, and tension at the blade tip are zero. At the blade root,  $\bar{x}_0 = 0$ , the boundry conditions for bending involve only geometric quantities, i.,e., the bending displaceements and slopes. The mixed boundry condition for torsion, Equation (B.5b), is a result of the root torsional spring.

Equations (B.1)- (B.6) are written in a general form which is most suitable when using the Galerkin finite element method to discretize the spatial dependence. All quantities appearing in these equations are defined below.

The elastic moments are given by:

$$M_3 = (\bar{EI}_2 \cos^2 R_c \theta_G + \bar{EI}_3 \sin^2 R_c \theta_G) \bar{V}_{,xx} + (\bar{EI}_2 - \bar{EI}_3) \left[ \left( \frac{1}{2} \bar{W}_{,xx} - \phi \bar{V}_{,xx} \right) \sin 2R_c \theta_G + \phi \bar{W}_{,xx} \cos 2R_c \theta_G \right] \quad (\text{B.7a})$$

$$M_2 = -(\bar{EI}_2 - \bar{EI}_3) \left[ \left( \frac{1}{2} \bar{V}_{,xx} + \phi \bar{W}_{,xx} \right) \sin 2R_c \theta_G + \phi \bar{V}_{,xx} \cos 2R_c \theta_G \right] - (\bar{EI}_2 \sin^2 R_c \theta_G + \bar{EI}_3 \cos^2 R_c \theta_G) \bar{W}_{,xx} \quad (\text{B.7b})$$

$$M_1 = (\bar{EI}_2 - \bar{EI}_3) \left[ \frac{1}{2} (\bar{V}_{,xx}^2 - \bar{W}_{,xx}^2) \sin 2R_c \theta_G - \bar{V}_{,xx} \bar{W}_{,xx} \cos 2R_c \theta_G \right] \quad (\text{B.7c})$$

$$M_x = \bar{GJ} (\phi_{,x} + \bar{V}_{,xx} \bar{W}_{,x}) \quad (\text{B.7d})$$

The distributed force and moment vectors, per unit length of the undeformed elastic axis, are expressed as:

$$\underline{p} = P_x \hat{e}_x + P_y \hat{e}_y + P_z \hat{e}_z \quad (\text{B.8a})$$

$$\underline{q} = q_x \hat{e}_x + q_y \hat{e}_y + q_z \hat{e}_z \quad (\text{B.8b})$$

In general, these loads contain inertia, aerodynamics, and structural damping contributions, denoted by the subscripts I, A and D, respectively. In writing the equations of motion, (B.1)-(B.4), the final form of the loads, Reference [2], has been used. Note,

however, that due to a more consistent applications of the ordering scheme, the torsional inertia load, Equation (B.10c) differs in some higher-order terms.

Inertia loads:

$$p_{xI} = \bar{m}(\bar{e}_1 + \bar{x}_0 + 2\bar{V}) \quad (\text{B.9a})$$

$$p_{yI} = \bar{m}(\bar{V} - \ddot{\bar{V}} + 2\beta_p \ddot{\bar{W}} - 2\ddot{\bar{U}} + \bar{x}_I \cos \theta_G + \bar{x}_I \ddot{\theta}_G \sin \theta_G) \quad (\text{B.9b})$$

$$p_{zI} = \bar{m}(-\beta_p(\bar{e}_1 + \bar{x}_0) - \ddot{\bar{W}} - 2\beta_p \dot{\bar{V}} - \bar{x}_I \ddot{\theta}_G \cos \theta_G) \quad (\text{B.9c})$$

$$\begin{aligned} q_{3I} &= -\bar{m}\bar{x}_I \cos \theta_G (\bar{e}_1 + \bar{x}_0) + \dot{\theta}_G (\bar{I}_{m2} - \bar{I}_{m3}) \sin 2\theta_G \\ &\cong q_{zI} \end{aligned} \quad (\text{B.10a})$$

$$\begin{aligned} q_{2I} &= \bar{m}\bar{x}_I \sin \theta_G (\bar{e}_1 + \bar{x}_0) - 2\dot{\theta}_G (\bar{I}_{m2} \sin^2 \theta_G + \bar{I}_{m3} \cos^2 \theta_G) \\ &\cong q_{yI} \end{aligned} \quad (\text{B.10b})$$

$$\begin{aligned} q_{1I} &= \bar{m}\bar{x}_I \left[ \sin \theta_G (\ddot{\bar{V}} - \bar{V} + \bar{V}_{,X}(\bar{e}_1 + \bar{x}_0)) \right. \\ &\quad + \cos \theta_G (-\beta_p + \bar{W}_{,X})(\bar{e}_1 + \bar{x}_0) - \ddot{\bar{W}} - 2\beta_p \dot{\bar{V}} \\ &\quad + \phi(\ddot{\bar{V}} - \bar{V}) + \phi \bar{V}_{,X}(\bar{e}_1 + \bar{x}_0) - 2\bar{W}_{,X} \dot{\bar{V}} \left. \right] - (\bar{I}_{m2} + \bar{I}_{m3}) \\ &\quad \cdot (\ddot{\theta}_G + \ddot{\phi} + \bar{W}_{,X} \ddot{\bar{V}}_{,X}) - (\bar{I}_{m2} - \bar{I}_{m3}) \\ &\quad \cdot \left[ \cos 2\theta_G (\phi - \beta_p \bar{V}_{,X} + 2\phi \dot{\bar{V}}_{,X}) + \sin 2\theta_G \left( \frac{1}{2} + \dot{\bar{V}}_{,X} \right) \right] \\ &\quad - (\bar{I}_{m2} \sin^2 \theta_G + \bar{I}_{m3} \cos^2 \theta_G) 2\bar{W}_{,X} (1 + \dot{\bar{V}}_{,X}) \\ &\cong \bar{V}_{,X} q_{yI} + \bar{W}_{,X} q_{zI} + q_{xI} \end{aligned} \quad (\text{B.10c})$$

Aerodynamic loads:

$$\begin{aligned}
 p_{yA} = -\Gamma & \left[ (\theta_G F_1 - F_2 + \dot{\theta}_G F_4) F_2 + \frac{C_{d0}}{a} \dot{F}_1^2 + \beta_P (\theta_G F_1 - 2F_2) \bar{V} \right. \\
 & + \left( \theta_G F_2 + 2 \frac{C_{d0}}{a} F_1 \right) F_3 \bar{V}_{,x} + (\theta_G F_1 - 2F_2 + \dot{\theta}_G F_4) F_3 \bar{W}_{,x} \\
 & + F_1 F_2 \phi + (\theta_G F_1 - 2F_2 - 2\beta_P F_3) \bar{V} \bar{W}_{,x} + (\theta_G F_3^2 + F_1 F_2) \bar{V}_{,x} \bar{W}_{,x} \\
 & - F_3^2 \bar{W}_{,x} \bar{W}_{,x} + (\beta_P F_1 \bar{V} + F_2 F_3 \bar{V}_{,x} + F_1 F_3 \bar{W}_{,x}) \dot{\phi} \\
 & + (-2\bar{V} + F_1 \bar{V}_{,x}) F_3 \bar{W}_{,x} \bar{W}_{,x} + (F_1 \bar{V} + F_3^2 \bar{V}_{,x}) \bar{W}_{,x} \phi \\
 & + \left( \theta_G F_2 + 2 \frac{C_{d0}}{a} F_1 \right) \dot{\bar{V}} + (\theta_G F_1 - 2F_2 + \dot{\theta}_G F_4) \dot{\bar{W}} + F_2 F_4 \dot{\phi} \\
 & + (\theta_G F_3 \bar{W}_{,x} + F_2 \phi) \dot{\bar{V}} + (\theta_G F_3 \bar{V}_{,x} - 2\beta_P \bar{V} - 2F_3 \bar{W}_{,x} + F_1 \phi) \dot{\bar{W}} \\
 & + F_3 F_4 \bar{W}_{,x} \dot{\phi} + F_3 \phi \bar{W}_{,x} \dot{\bar{V}} + (-2\bar{V} \bar{W}_{,x} + F_1 \bar{V}_{,x} \bar{W}_{,x} + F_3 \phi \bar{V}_{,x}) \dot{\bar{W}} \\
 & \left. + \theta_G \dot{\bar{W}} \dot{\bar{V}} - \dot{\bar{W}} \dot{\bar{W}} + F_4 \dot{\bar{W}} \dot{\phi} + \phi \dot{\bar{W}} \dot{\bar{V}} \right]
 \end{aligned} \tag{B.11a}$$

$$\begin{aligned}
 p_{zA} = -\Gamma & \left[ (-\theta_G F_1 + F_2 - \dot{\theta}_G F_4) F_1 + \beta_P F_1 \bar{V} + (F_2 - 2\theta_G F_1) F_3 \bar{V}_{,x} \right. \\
 & + F_1 F_3 \bar{W}_{,x} - F_1^2 \phi + F_1 \bar{V} \bar{W}_{,x} + (F_3^2 - F_1^2) \bar{V}_{,x} \bar{W}_{,x} \\
 & - 2F_1 F_3 \bar{V}_{,x} \phi + (F_2 - 2\theta_G F_1) \dot{\bar{V}} + F_1 \dot{\bar{W}} - F_1 F_4 \dot{\phi} \\
 & \left. + (F_3 \bar{W}_{,x} - 2F_1 \phi) \dot{\bar{V}} + F_3 \bar{V}_{,x} \dot{\bar{W}} + \dot{\bar{V}} \dot{\bar{W}} \right]
 \end{aligned} \tag{B.11b}$$

$$\begin{aligned}
 q_{xA} = -\Gamma b^{-2} \frac{R^2}{l^2} & (0,5 - \bar{x}_A)(1 - \bar{x}_A)(\dot{\theta}_G + \dot{\phi}) F_1 \\
 & - \Gamma b^{-2} \frac{R}{l} \bar{x}_A \left[ (F_2 - \theta_G F_1) F_1 + \beta_P F_1 \bar{V} + (F_2 - 2\theta_G F_1) F_3 \bar{V}_{,x} \right. \\
 & + F_1 F_3 \bar{W}_{,x} - F_1^2 \phi + F_1 \bar{V} \bar{W}_{,x} + (F_3^2 - F_1^2) \bar{V}_{,x} \bar{W}_{,x} \\
 & \left. - 2F_1 F_3 \bar{V}_{,x} \phi + (F_2 - 2\theta_G F_1) \dot{\bar{V}} + F_1 \dot{\bar{W}} \right]
 \end{aligned}$$

$$F_3 \bar{W}_{,x} \dot{\bar{V}} - 2F_1 \phi \dot{\bar{V}} + F_3 \bar{V}_{,x} \dot{\bar{W}} + \dot{\bar{V}} \dot{\bar{W}} \Big] \quad (\text{B.11c})$$

$$F_1 = \bar{e}_1 + \bar{x}_0 + \mu \frac{R}{l} \sin \psi \quad (\text{B.11d})$$

$$F_2 = \lambda \frac{R}{l} + \mu \frac{R}{l} \beta_p \cos \psi \quad (\text{B.11e})$$

$$F_3 = \mu \frac{R}{l} \cos \psi \quad (\text{B.11f})$$

$$F_4 = b \frac{R}{l} (1,5 - \bar{x}_A) \quad (\text{B.11g})$$

$$F_5 = b^{-2} \frac{R^2}{l^2} (0,5 - \bar{x}_A)(1 - \bar{x}_A) \quad (\text{B.11h})$$

Damping loads:

$$p_{yD} = -\bar{g}_{SL} \dot{\bar{V}} \quad (\text{B.12a})$$

$$p_{zD} = -\bar{g}_{SF} \dot{\bar{W}} \quad (\text{B.12b})$$

$$q_{xD} = -\bar{g}_{ST} \dot{\phi} \quad (\text{B.12c})$$

The coupled flap-lag-torsion problem is thus defined by Equations (B.2) – (B.4), together with the elastic moment, Equations (B.7), and the loads, Equations (B.9) – (B.12). Note, that the tension  $\bar{T}$  will be eliminated using the axial equation and corresponding boundary condition, Equations (B.1) and (B.6d). The axial displacement,  $\bar{u}$ , will be replaced using the assumption that the blade is inextensional in the axial direction, an assumption which is commonly made in rotary-wing aeroelasticity.

## APPENDIX\_C

### C.1 LINEER UNDAMPED DYNAMIC EQUATION :

$$[I_1^e] \ddot{a} + ([B_1^e] + [T_1^e] + [K_1^e] + [A_1^e]) \dot{a} = -\{F_1^e\} - \{F_A^e\}$$

$$\gamma = \eta = \begin{bmatrix} 1 - 3 \frac{x_e^2}{L_e^2} + 2 \frac{x_e^3}{L_e^3} \\ x_e - 2 \frac{x_e^2}{L_e} + \frac{x_e^3}{L_e^2} \\ 3 \frac{x_e^2}{L_e^2} - 2 \frac{x_e^3}{L_e^3} \\ -\frac{x_e^2}{L_e} + \frac{x_e^3}{L_e^2} \end{bmatrix} \quad \Phi = \begin{bmatrix} 1 - 3 \frac{x_e^2}{L_e^2} + 2 \frac{x_e^3}{L_e^3} \\ 4 \frac{x_e^2}{L_e} - 4 \frac{x_e^3}{L_e^2} \\ -\frac{x_e^2}{L_e} + 2 \frac{x_e^3}{L_e^2} \end{bmatrix}$$

$$X_0 = r_e + x_e$$

$$[A_1^e] = \Gamma \begin{bmatrix} r \gamma^T \beta_p (\theta_o F_1 - 2 F_2) \\ + \gamma \gamma_x^T \left( \theta_o F_2 + 2 \frac{C_{\omega}}{a} F_1 \right) F_3 & \gamma \eta_x^T (\theta_o F_1 - 2 F_2 + \theta_o F_4) F_3 & \gamma \phi^T F_1 F_2 \\ \eta \gamma^T \beta_p F_1 \\ + \eta \gamma_x^T (F_2 - 2 \theta_o F_1) F_3 & \eta \eta_x^T F_1 F_3 & -\eta \phi^T F_1^2 \\ \bar{b} \frac{R}{l} \bar{x}_\lambda \left( \phi \gamma^T F_1 + \phi \gamma_x^T (F_2 - 2 \theta_o F_1) F_3 \right) & \phi \eta_x^T \bar{b} \frac{R}{l} \bar{x}_\lambda F_1 F_3 & -\phi \phi^T \bar{b} \frac{R}{l} \bar{x}_\lambda F_1^2 \end{bmatrix}$$

$$[B_1] = \int_0^{L_e} \begin{bmatrix} \gamma_{,xx} \gamma_{,xx}^T B_{22} & \gamma_{,xx} \eta_{,xx}^T B_{23} & 0 \\ \eta_{,xx} \gamma_{,xx}^T B_{23} & \eta_{,xx} \eta_{,xx}^T B_{33} & 0 \\ 0 & 0 & \phi_{,x} \phi_{,x}^T GJ \end{bmatrix}$$

$$[F_I] = \int_0^{L_e} \left\{ \begin{array}{l} -\gamma(x_{ic} + x_{is} \ddot{\theta}_G) + \gamma_{,x} [x_{ic} (\bar{e}_I + \bar{x}_0) - B_{m23} \dot{\theta}_G] \\ \eta [\bar{m} \beta_p (e_1 + x_0) + x_{ic} \ddot{\theta}_G] + \eta_{,x} [x_{is} (e_1 + x_0) - B_{m33} \dot{\theta}_G] \\ \phi [x_{ic} \beta_p (e_1 + x_0) + \frac{1}{2} B_{m23} + B_{m0} \ddot{\theta}_G] \end{array} \right\} d_{xe}$$

$$\{F_A\} = \Gamma \int_0^{L_e} \left\{ \begin{array}{l} \gamma (\theta_G F_1 - F_2 + \dot{\theta}_G F_4) F_2 + \frac{C_{d0}}{a} F_1^2 \\ \eta (-\theta_G F_1 + F_2 - \dot{\theta}_G F_4) F_1 \\ \phi \left[ \bar{b} \frac{R}{L} X_A (F_2 - \theta_G F_1) F_1 + \dot{\theta}_G F_1 F_5 \right] \end{array} \right\} d_{xe}$$

$$[L_1] = \int_0^{L_e} \begin{bmatrix} \gamma \gamma^T \bar{m} & 0 & 0 \\ 0 & \eta \eta^T \bar{m} & 0 \\ -\phi \gamma^T x_{is} & \phi \eta^T x_{ic} & \phi \phi^T B_{m0} \end{bmatrix} d_{xe}$$

$$[T_1] = \int_0^{L_e} \begin{bmatrix} \gamma_{,x} \gamma_{,x}^T T_1 & 0 & 0 \\ 0 & \eta_{,x} \eta_{,x}^T T_1 & 0 \\ 0 & 0 & 0 \end{bmatrix} d_{xe}$$

## **CIRCULURIUM VITA**

She was born in Bursa in 1970. She was graduated from Balabanbey Primary School and Bursa Girls School. In 1990, she has studied at The Mechanical Engineering Department of Engineering Faculty in Uludağ University. In 1994, she graduated from the mechanical engineering department by taking a second class honours degree. In the same year, she has begun to study to get Master's degree in The Mechanical Faculty of Istanbul Technical University. Still, she's working in a computer company as a CAD/CAM engineer.

